Site-specific effects of neurosteroids on GABA$_A$ receptor activation and desensitization

Yusuke Sugasawa[1], Wayland W. L. Cheng[1], John R. Bracamontes[1], Zi-Wei Chen[1,5], Lei Wang[1],

Allison L. Germann[1], Spencer R. Pierce[1], Thomas C. Senneff[1], Kathiresan Krishnan[2],

David E. Reichert[3,5], Douglas F. Covey[1,2,4,5], Gustav Akk[1,5], Alex S. Evers[1,2,5*]

From the Departments of [1]Anesthesiology, [2]Developmental Biology, [3]Radiology, [4]Psychiatry, and the [5]Taylor Family Institute for Innovative Psychiatric Research, Washington University in St. Louis, St. Louis, Missouri 63110.

[*]To whom correspondence should be addressed: Professor Alex S. Evers, Department of Anesthesiology, Washington University School of Medicine, Campus Box 8054, St. Louis, Missouri 63110. Telephone: (314) 454-8701; Fax: (314) 454-5572; E-mail: eversa@wustl.edu

Yusuke Sugasawa	sugasaway@wustl.edu
Wayland W. L. Cheng	wayland.cheng@wustl.edu
John R. Bracamontes	jbracamontes@wustl.edu
Zi-Wei Chen	chenziwei@wustl.edu
Lei Wang	leiwang@wustl.edu
Allison L. Germann	germanna@wustl.edu
Spencer R. Pierce	spencerp@wustl.edu
Thomas C. Senneff	tcsenneff@wustl.edu
Kathiresan Krishnan	krishnan@wustl.edu
David E. Reichert	reichertd@wustl.edu
Douglas F. Covey	dcovey@wustl.edu
Gustav Akk	akk@wustl.edu

1 ABSTRACT

2 This study examines how site-specific binding to the three identified neurosteroid binding sites in the

3 $\alpha_1\beta_3$ GABA$_A$ receptor (GABA$_A$R) contributes to neurosteroid allosteric modulation. We found that the

4 potentiating neurosteroid, allopregnanolone, but not its inhibitory 3β-epimer epi-allopregnanolone, binds

5 to the canonical $\beta_3(+)-\alpha_1(-)$ intersubunit site that mediates receptor activation by neurosteroids. In contrast,

6 both allopregnanolone and epi-allopregnanolone bind to intrasubunit sites in the β_3 subunit, promoting

7 receptor desensitization and the α_1 subunit promoting ligand-specific effects. Two neurosteroid analogues

8 with diazirine moieties replacing the 3-hydroxyl (KK148 and KK150) bind to all three sites, but do not

9 potentiate GABA$_A$R currents. KK148 is a desensitizing agent, whereas KK150 is devoid of allosteric

10 activity. These compounds provide potential chemical scaffolds for site-specific and general neurosteroid

11 antagonists. Collectively, these data show that differential occupancy and efficacy at three discrete

12 neurosteroid binding sites determine whether a neurosteroid has potentiating, inhibitory, or competitive

13 antagonist activity on GABA$_A$Rs.

14

15

16

19

20

1 INTRODUCTION

2 Neurosteroids (NS) are endogenous modulators of brain development and function and are important

3 mediators of mood (1-4). Exogenously administered NS analogues have been clinically used as anesthetics

4 and anti-depressants and have therapeutic potential as anti-epileptics, neuroprotective agents and cognitive

5 enhancers (1,2,5-9). The principal target of NS is the γ-aminobutyric acid type A receptor (GABA$_A$R). NS

6 can either activate or inhibit GABA$_A$Rs. Positive allosteric modulatory NS (PAM-NS) such as

7 allopregnanolone (3α5αP) potentiate the effect of GABA on GABA$_A$R currents at low concentrations and

8 directly activate the receptors at higher concentrations (5,10-12). Negative allosteric modulatory NS

9 (NAM-NS), such as epi-allopregnanolone (3β5αP) or pregnenolone sulfate (PS) inhibit GABA$_A$R currents

10 (13-17). In addition to enhancing channel opening, PAM-NS increase the affinity of the GABA$_A$R for

11 orthosteric ligand binding, an effect thought to be mechanistically linked to channel gating (11,18).

12

13 GABA$_A$Rs are pentameric ligand-gated ion channels (pLGIC) composed of two α-subunits (α$_{1-6}$), two

14 β-subunits (β$_{1-3}$) and one additional subunit (γ$_{1-3}$, δ, ε, θ or π) (19-21). Each subunit is composed of a large

15 extracellular domain (ECD), a transmembrane domain (TMD) formed by four membrane-spanning helices

16 (TM1-4), a long intracellular loop between TM3 and TM4, and a short extracellular C-terminus (5,19,20,22).

17 NS modulate GABA$_A$Rs by binding to sites within the TMDs (1,2,5,6,11,23-28). Specifically, the α subunit

18 TMDs are essential to the actions of PAM-NS (11,23,24,27,28). Mutagenesis studies in α$_1$β$_2$γ$_2$ GABA$_A$Rs

19 have identified several residues in the α$_1$ subunit, notably Q242 and W246 in TM1, as critical to NS

20 potentiation of GABA-elicited currents (25,26,29). Crystallographic studies have subsequently shown that,

21 in homo-pentameric chimeric receptors in which the TMDs are derived from either α$_1$ (24,27) or α$_5$ subunits

22 (23), the NS 3α,21dihydroxy-5α-pregnan-20-one (3α5α-THDOC), pregnanolone and alphaxalone bind in a

23 cleft between the α subunits, with the C3-hydroxyl substituent of the steroids interacting directly with Q242

24 in the α subunit (αQ242). PAM-NS activate these chimeric receptors, and their action is blocked by αQ242L

25 and αQ242W mutations. These studies posit a single canonical intersubunit binding site for NS action that

1   is conserved across the six α subunit isoforms (23,24,27).

2

3   An alternative body of evidence suggests that PAM-NS modulation of GABA$_A$R function is mediated

4   by multiple mechanisms and/or binding sites. Site-directed mutagenesis has identified multiple disparate

5   residues on GABA$_A$Rs that affect NS-induced activation, suggestive of two neurosteroid binding sites; one

6   site mediating potentiation of GABA responses and the other mediating direct activation (25,26). Single

7   channel electrophysiological studies (5,10,30) as well as studies examining neurosteroid modulation of

8   [^{35}S]t-butylbicyclophosphorothionate (TBPS) binding (31), have also identified multiple distinct effects of

9   NS, with various structural analogues producing some or all of these effects, consistent with multiple NS

10   binding sites (25,26). Our recent photolabeling studies have confirmed that there are multiple PAM-NS

11   binding sites on α$_1$β$_3$ GABA$_A$Rs (11). In addition to the canonical site at the interface between the TMDs

12   of adjacent subunits (intersubunit site) (11,23,24,27), we identified NS binding sites within the α-helical

13   bundles of both the α$_1$ and β$_3$ subunits (intrasubunit sites) of α$_1$β$_3$ GABA$_A$Rs (11). 3α5αP binds to all three

14   sites (11); mutagenesis of these sites suggests that the intersubunit and α$_1$ intrasubunit sites, but not the β$_3$

15   intrasubunit site, contribute to 3α5αP PAM activity (11). A functional effect for NS binding to the β$_3$

16   intrasubunit site has not been identified.

17

18   The 3α-hydroxyl (3α-OH) group is critical to NS activation of GABA$_A$Rs and 3β-OH NS lack PAM

19   activity (5,14). Indeed, many 3β-OH NS are GABA$_A$R NAMs (14,16). While molecular docking studies

20   have suggested that the 3β-OH NS epi-pregnanolone competes for binding with PAM-NS (23), 3β-OH NS

21   are non-competitive inhibitors with respect to GABA and 3α-OH NS, indicating that they are unlikely to

22   act at the canonical PAM binding site (5,14). Steroids with a sulfate rather than a hydroxyl at the 3-carbon

23   are also GABA$_A$R NAMs thought to act at sites distinct from GABA$_A$R PAMs (5,13,14,17,32). The precise

24   location of this site is unclear, but crystallographic studies have demonstrated a possible binding site

25   between TM3 and TM4 on the intracellular end of the α-subunit TMD (17,24). While 3β-OH NS and PS

26   both inhibit GABA$_A$Rs, they likely act via interactions with distinct sites (5,13,14,16,17,23,24).

1

2   The goal of the current study was to determine the specific sites underlying the PAM and NAM actions

3   of NS. We hypothesized that various NS analogues preferentially bind to one or more of the three NS

4   binding sites in the $\alpha_1\beta_3$ GABA$_A$R, stabilizing distinct conformational states (i.e. resting, open or

5   desensitized). To achieve this goal, we used two endogenous NS, the PAM-NS 3α5αP and the NAM-NS

6   3β5αP and two NS analogues, KK148 and KK150, in which a diazirine replaced the function-critical 3-OH

7   group (33). We examined site-specific NS binding and effects using NS photolabeling (28,34-36) and

8   measurements of channel gating and orthosteric ligand binding. The NS lacking a 3α-OH were devoid of

9   PAM-NS activity, but surprisingly, KK148 and 3β5αP enhanced the affinity of [^{3}H]muscimol binding. We

10   interpret this finding as evidence that these compounds preferentially bind to and stabilize desensitized

11   receptors, since both open and desensitized GABA$_A$R exhibit enhanced orthosteric ligand binding affinity

12   (37).

13

14   The results show that 3α5αP binds to the canonical β(+)–α(-) intersubunit site, stabilizing the open state

15   of the receptor, whereas the 3-diazirinyl NS (KK148 and KK150) bind to this site but do not promote

16   channel opening, and 3β5αP does not occupy this site. These data indicate that NS binding to the

17   intersubunit sites is largely responsible for PAM activity and that the 3α-OH is critical for NS activation. In

18   contrast, 3α5αP, 3β5αP and the 3-diazirinyl NS all bind to both the α_1 and β_3 intrasubunit sites. Occupancy

19   of the intrasubunit sites by 3α5αP, 3β5αP and KK148 promotes receptor desensitization. KK150 occupies

20   all three NS binding sites on $\alpha_1\beta_3$ GABA$_A$Rs, but produces minimal functional effect suggesting a possible

21   scaffold for a general NS antagonist. These results shed new light on the mechanisms of NS allosteric

22   modulation of channel function, and demonstrate a novel pharmacology in which related ligands bind to

23   different subsets of functional sites on the same protein, each in a state-dependent manner, with the actions

24   at these sites summating to produce a net physiological effect.

25

1 **RESULTS**

2 *Distinct patterns of NS potentiation and enhancement of muscimol binding.*

3   The endogenous NS, 3α5αP is known to potentiate GABA-elicited currents (Figure 1A) and enhance

4 [^{3}H]muscimol binding to $\alpha_1\beta_3$ GABA$_A$Rs (Figure 1E) (11,18). We examined a series of NS analogues with

5 different stereochemistries or substituents in the 3- and 17-positions: 3β5αP, KK148, and KK150 (structures

6 shown in Figures 1B-D) for their ability to potentiate GABA-elicited currents and enhance orthosteric

7 agonist ([^{3}H]muscimol) binding. 3β5αP is the 3β-epimer of 3α5αP. KK148 and KK150 are NS analogue

8 photolabeling reagents, which have a 3-diazirinyl moiety instead of the 3-OH, and differ from each other

9 by the stereochemistry of the 17-ether linkage (33). We observed a discrepancy between the ability of these

10 compounds to potentiate GABA-elicited currents and their ability to enhance [^{3}H]muscimol binding in $\alpha_1\beta_3$

11 GABA$_A$Rs. None of the NS analogues lacking a 3α-OH potentiated GABA-elicited currents (Figures 1B-

12 D). However, both 3β5αP and KK148 significantly enhanced [^{3}H]muscimol binding (Figure 1E). KK150,

13 in contrast, did not potentiate GABA-elicited currents and minimally enhanced [^{3}H]muscimol binding

14 (Figures 1D-E). Collectively, these data show that, NS analogues with different stereochemistry or

15 substituents at the 3- and 17-positions show distinct patterns in modulation of $\alpha_1\beta_3$ GABA$_A$R currents and

16 orthosteric ligand binding. We hypothesized that these patterns are a consequence of the various NS

17 analogues stabilizing distinct conformational states of the GABA$_A$R, possibly by binding and acting at

18 different sites. Notably, the compounds with a 3-OH (3α5αP, 3β5αP) are ten-fold more potent than those

19 with a 3-diazirine (KK148, KK150) in enhancing [^{3}H]muscimol binding (Figure 1E), suggesting that the 3-

20 OH is an important determinant of binding affinity to the site(s) mediating these effects.

21

22 *State-specific actions of NS analogues.*

23   To determine why 3β5αP and KK148 enhance [^{3}H]muscimol binding but do not potentiate $\alpha_1\beta_3$

24 GABA$_A$R currents, we first considered the possibility that 3β5αP- and KK148-induced enhancement of

25 [^{3}H]muscimol binding is a selective effect on intracellular GABA$_A$Rs, since the radioligand binding assay

26 was performed on total membrane homogenates, whereas the electrophysiological assays report only from

1   cell surface channels. NS are known to have effects on intracellular $GABA_A$Rs and have been shown to

2   accelerate $GABA_A$R trafficking (38-40). To test this possibility, we examined [³H]muscimol binding in

3   intact cells (i.e. binding to receptors only in the plasma membrane) (41-43) compared to permeabilized cells

4   (plasma membranes plus intracellular membranes). Notably, [³H]muscimol binding was two-fold greater in

5   permeabilized cells than in intact cells, indicating a significant population of intracellular $GABA_A$Rs.

6   KK148 enhanced [³H]muscimol binding in intact cells as much or more than in permeabilized cells,

7   indicating that this effect is not a result of selective NS actions on intracellular receptors (Figure 1–figure

8   supplement 1).

9

10 A second possibility is that 3β5αP and KK148 selectively bind to and stabilize a desensitized state of

11 the $GABA_A$R. This would result in enhanced [³H]muscimol binding, since both open and desensitized

12 receptors exhibit increased orthosteric ligand affinity in comparison to the resting state (11,18,37). To

13 examine the effect of these NS analogues on desensitization, we maximally activated $α_1β_3$ $GABA_A$R with

14 1 mM GABA and tested the effect of the NS on steady-state currents (44). KK148 and 3β5αP both decreased

15 steady-state currents (Figures 2A and 2C), whereas KK150 did not (Figure 2B). To further delineate the

16 electrophysiological effects of these compounds we focused on 3β5αP, since it is an endogenous NS and

17 we had limited availability of KK148. 3β5αP preferentially inhibited steady-state rather than peak currents,

18 indicating that inhibition is unlikely to be a rapidly-developing channel blocking effect. The inhibitory

19 effect was also not observed in the $α_1$(V256S)$β_3$ TM2 pore-lining mutation, which was previously shown

20 to remove the desensitizing effects of sulfated steroids (13,14) (Figure 2D). While both 3α5αP and 3β5αP

21 enhance [³H]muscimol binding, the former predominantly results in receptor activation while the latter

22 results in desensitization. Consistent with this, the $α_1$(V256S)$β_3$ mutation which abolishes NS-induced

23 desensitization (13,14) eliminated [³H]muscimol binding enhancement by 3β5αP but not 3α5αP (Figure 3).

24 We infer that 3α5αP increases [³H]muscimol binding by stabilizing an active state of the receptor, whereas

25 3β5αP increases [³H]muscimol binding by stabilizing a desensitized state of the receptor which is absent in

26 the $α_1$(V256S)$β_3$ receptor. Collectively, these data indicate that 3β5αP and KK148 stabilize a desensitized

1   state of the $GABA_AR$, thus enhancing orthosteric ligand affinity.

2

3   ***Quantitative comparison of the effects of 3β5αP on [³H]muscimol binding and receptor desensitization.***

4   While there is qualitative agreement between the relative effects of the various NS analogues on

5   orthosteric ligand binding and receptor desensitization, there is an apparent quantitative discrepancy in the

6   magnitude of the effects. For example, 3β5αP enhances [³H]muscimol binding by two-fold (Figure 1E),

7   whereas it reduces steady-state current by only ~25% (Figure 2C). To address this difference, we first

8   considered that the radioligand binding and electrophysiological assays are performed under different

9   experimental conditions. The radioligand binding studies are performed using low [³H]muscimol

10   concentrations to allow for sufficient dynamic range of ligand binding. In contrast the desensitization

11   experiments are performed at high orthosteric ligand (GABA) concentration to achieve high peak open

12   probability and steady-state receptor desensitization, thus minimizing the number of channels in the resting

13   state. To address the quantitative differences in results from the two assays, we analyzed the

14   electrophysiological data in the framework of the three-state Resting-Open-Desensitized model (44,45).

15   We assumed that both the open and desensitized states had higher affinity for muscimol than the resting

16   state, and that the affinities were similar and could be treated as equal. We then calculated the predicted

17   occupancy of the high affinity states (P_{open} + $P_{desensitized}$) using parameters derived from the functional

18   responses, to compare to the observed changes in binding. The raw current amplitudes of peak and steady-

19   state responses were converted to units of open probability as described previously in detail (46), and the

20   probabilities of being in the open (P_{open}) or desensitized ($P_{desensitized}$) states were calculated for different

21   experimental conditions (see Methods).

22

23   Application of 1 mM GABA elicited a current response that had a peak P_{open} of 0.71 ± 0.25 ($n = 16$).

24   The P_{open} of the steady-state response was 0.121 ± 0.033 ($n = 7$), that was reduced to 0.077 ± 0.013 ($n = 5$)

25   with 3 µM 3β5αP. Analysis of steady-state currents using the Resting-Open-Desensitized model indicates

26   that the steady-state $P_{desensitized}$ is 0.829 in the presence of GABA, and 0.892 in the presence of GABA +

1   steroid. The relatively small increase in the sum of (P_{open} + $P_{desensitized}$) (from 0.95 to 0.97) is due to the use

2   of saturating GABA in these experiments. In the presence of lower concentrations of GABA, i.e., lower

3   levels of activation, the predicted increase in the sum of (P_{open} + $P_{desensitized}$) is greater. For example, for the

4   condition where GABA elicits a peak response with P_{open} of 0.01, the predicted steady-state P_{open} is 0.0094

5   and the predicted $P_{desensitized}$ 0.0643 (sum of the two equals 0.0737). In the presence of GABA + 3β5αP, the

6   predicted steady-state P_{open} is 0.0090 and the predicted $P_{desensitized}$ 0.1045 (sum of 0.1135), thus showing a

7   54% increase in the sum of (P_{open} + $P_{desensitized}$). Incidentally, this example demonstrates the need to use high

8   concentrations of GABA to observe a meaningful reduction in steady-state P_{open} in the presence of 3β5αP.

9

10   To more directly compare the data from the radioligand binding and electrophysiology experiments, we

11   exposed oocytes containing $\alpha_1\beta_3$ GABA$_A$Rs to 20 nM muscimol and recorded currents before and after co-

12   application of 3 μM 3β5αP. The percent reduction in steady-state current following 3β5αP exposure was

13   measured and used to estimate the relative probabilities of closed, open and desensitized receptors. The

14   application of 20 nM muscimol elicited a peak response with P_{open} of 0.012 ± 0.004 (*n* = 6). The steady-

15   state P_{open} was 0.011 ± 0.004. In the same cells, subsequent exposure to 3 μM 3β5αP reduced the steady-

16   state P_{open} to 0.009 ± 0.004. The calculated steady-state $P_{desensitized}$ was 0.1001 in the presence of muscimol,

17   and 0.2168 in the presence of muscimol + 3β5αP. Thus, there is a predicted two-fold increase in the sum of

18   (P_{open} + $P_{desensitized}$) when the steroid is combined with muscimol. This is consistent with the doubling of

19   muscimol binding caused by 3β5αP in the [^{3}H]muscimol binding experiments (Figure 1E). Overall, the data

20   indicate that relatively small changes in steady-state current can be associated with relatively large changes

21   in the occupancy of high-affinity states.

22

23   ***Binding site selectivity for NS analogues.***

24   To determine whether KK148 and 3β5αP stabilize the desensitized conformation of the GABA$_A$R by

25   selectively binding to one or more of the identified NS binding sites on the GABA$_A$R (11), we first

26   determined which of the identified NS sites they bind. We have previously shown that the 3α5αP-analogue

1   photolabeling reagent, KK200 labels the $\beta_3(+)$–$\alpha_1(-)$ intersubunit (β_3G308) and α_1 intrasubunit (α_1N408)

2   sites on $\alpha_1\beta_3$ GABA$_A$Rs (Figure 4A), and that photolabeling can be prevented by a ten-fold excess of $3\alpha5\alpha$P

3   (11). As a first step to determine the binding sites for $3\beta5\alpha$P, KK148 or KK150, we examined whether a

4   ten-fold excess of these compounds (30 μM) prevented KK200 (3 μM) photolabeling of either binding site.

5   Photolabeling was performed on membranes from HEK293 cells transfected with epitope-tagged α_{1His-}

6    $_{FLAG}\beta_3$ receptors, mimicking the conditions used in the [^{3}H]muscimol binding assays and photolabeled

7   residues were identified and labeling efficiency was determined using middle-down mass spectrometry (11).

8   KK148, KK150, $3\alpha5\alpha$P and $3\beta5\alpha$P all prevented KK200 photolabeling of α_1N408 in the α_1 intrasubunit site

9   (Figure 4B), consistent with their binding to this site. In contrast, KK148, KK150 and $3\alpha5\alpha$P but not $3\beta5\alpha$P

10   prevented labeling of β_3G308 in the intersubunit site (Figure 4C), indicating that $3\beta5\alpha$P does not bind to

11   the intersubunit site.

12

13   The KK148- and KK150-photolabeled samples were also analyzed to directly identify the sites of

14   adduction. In both the KK148- and KK150-labeled samples, photolabeled peptides were identified from

15   the TM4 helices of both the α_1 and β_3 subunits. The labeled peptides had longer chromatographic elution

16   times than the corresponding unlabeled peptides and corresponded with high mass accuracy (< 20 ppm) to

17   the predicted mass of the unlabeled peptides plus the add weight minus N_2 of KK148 or KK150 (Figure 4–

18   figure supplement 1). Product ion (MS2) spectra of the KK148- and KK150-labeled peptides from the α_1

19   subunit identified the labeled residue as Y415 for both KK148 and KK150 (Figures 4D-E, Figure 4–figure

20   supplement 2); Y415 is the same residue labeled by KK123 at the α_1 intrasubunit site (11). The KK148 and

21   KK150 labeled peptides in TM4 of the β_3 subunit and corresponding unlabeled peptide were identified by

22   fragmentation spectra as β_3TM4 I426-N445. These data support labeling of the β_3 intrasubunit site by

23   KK148 and KK150. Fragmentation spectra of the peptide-sterol adducts were not adequate to determine

24   the precise labeled residue because of low photolabeling efficiency (0.13% for KK148; 0.19% for KK150,

25   Figure 4–figure supplement 1). No photolabeled peptides were identified in the $\beta_3(+)$–$\alpha_1(-)$ intersubunit site.

26   This is likely because KK148 and KK150, similar to KK123, utilize an aliphatic diazirine that preferentially

1 labels nucleophilic residues (28,34,47); such residues are not present in the intersubunit site.

2

3   We have also shown that KK123 labeling of the α_1 intrasubunit (α_1Y415) and β_3 intrasubunit (β_3Y442)

4 sites (Figure 5A) can be prevented by a ten-fold excess of 3α5αP (11). We thus examined whether 3β5αP

5 (30 μM) inhibited photolabeling by KK123 (3 μM). 3β5αP completely inhibited KK123 photolabeling at

6 both intrasubunit sites (Figures 5B-C). Collectively the data show that KK148, KK150 and 3α5αP bind to

7 all three of the identified NS binding sites. In contrast, 3β5αP selectively binds to the two intrasubunit

8 binding sites, but not to the canonical β_3(+)–α_1(-) intersubunit site.

9

10 ***Orthosteric ligand binding enhancement by NS analogues is mediated by distinct sites.***

11   To determine which of the previously identified binding sites contributes to NS enhancement of

12 [3H]muscimol binding, we performed site-directed mutagenesis of the NS binding sites previously

13 determined by photolabeling (Figure 6A) (11). Specifically, α_1(Q242L)β_3 targets the β_3(+)–α_1(-)

14 intersubunit site, α_1(N408A/Y411F)β_3 and α_1(V227W)β_3 the α_1 intrasubunit site, and $\alpha_1\beta_3$(Y284F) the β_3

15 intrasubunit site. Mutations in the β_3(+)–α_1(-) intersubunit and α_1 intrasubunit sites decreased 3α5αP

16 enhancement of [3H]muscimol binding by ~80%, while mutation of the β_3 intrasubunit site led to a small

17 decrease (Figure 6B, Table 1). The residual enhancement of [3H]muscimol binding observed in receptors

18 with mutations in the intersubunit or α_1 intrasubunit site occurs at ten-fold higher concentrations of 3α5αP

19 than WT and receptors with mutations in the β_3 intrasubunit site (Table 1), suggesting that 3α5αP binds to

20 the β_3 intrasubunit site with lower affinity. In contrast, mutations in the α_1 and β_3 intrasubunit sites, but not

21 the intersubunit site decreased the enhancement of [3H]muscimol binding by 3β5αP and KK148 (Figures

22 6C-D, Table 1). To confirm that the effect of these mutations on NS effect are steroid-specific, we also

23 tested their effect on etomidate, which enhances [3H]muscimol binding in $\alpha_1\beta_3$ GABA$_A$Rs and acts through

24 a binding site distinct from NS (48,49). The mutations targeting NS binding sites resulted in modest

25 decreases in [3H]muscimol binding enhancement by etomidate; however, the $\alpha_1\beta_3$(M286W) mutation which

26 abolishes etomidate potentiation and activation of GABA$_A$Rs (50,51), also abolished [3H]muscimol binding

1   enhancement (Figure 6E).

2

3   We did not test the effects of mutations on KK150 action because it minimally enhances [^{3}H]muscimol

4   binding. However, KK150 binds to all three of the identified NS binding sites, and may thus be a weak

5   partial agonist or antagonist at the sites mediating NS enhancement of [^{3}H]muscimol binding. Consistent

6   with this prediction, KK150 inhibited enhancement of [^{3}H]muscimol binding by 3α5αP and KK148 (Figure

7   7).

8

9   Collectively, these results show that multiple NS binding sites contribute to enhancement of

10   [^{3}H]muscimol affinity and that potentiating NS (3α5αP) and non-potentiating NS (3β5αP, KK148 and

11   KK150) have both common and distinct sites of action. Specifically, 3α5αP enhances [^{3}H]muscimol binding

12   through all three sites but predominantly through the intersubunit and α$_1$ intrasubunit sites, which we have

13   previously shown mediate PAM-NS potentiation (11). In contrast, 3β5αP and KK148 enhance

14   [^{3}H]muscimol binding exclusively through the α$_1$ and β$_3$ intrasubunit sites. KK150 antagonizes the effects

15   of KK148 on [^{3}H]muscimol binding, presumably via the intrasubunit sites, and antagonizes the effects of

16   3α5αP, possibly via all three sites. These data indicate that NS binding to both the intersubunit and

17   intrasubunit sites contributes to 3α5αP enhancement of [^{3}H]muscimol binding, but that only the intrasubunit

18   binding sites contribute to the effects of 3β5αP and KK148.

19

20   It is important to note that the [^{3}H]muscimol binding curves in Figure 6 are normalized to control. The

21   raw data show that membranes containing WT receptors have 10-20-fold higher [^{3}H]muscimol binding

22   (B_{max}) than membranes containing α$_1$(N408A/Y411F)β$_3$ receptors (Figure 6–figure supplement 1A). The

23   lower total [^{3}H]muscimol binding observed in α$_1$(N408A/Y411F)β$_3$ membranes is likely a consequence of

24   decreased receptor expression. To assure that differences in NS effect between WT and α$_1$(N408A/Y411F)β$_3$

25   are not due to different muscimol affinities, we examined [^{3}H]muscimol binding at a full range of

26   concentrations. The α$_1$(N408A/Y411F)β$_3$ mutations did not have a significant effect on [^{3}H]muscimol

1   affiliity (Figure 6–figure supplement 1B), but eliminated the modulatory effects of NS (3α5αP and KK148)

2   on [^{3}H]muscimol affinity (Figure 6–figure supplement 1C-D and Figure 6–figure supplement 2). To assure

3   that the effect of α_1(N408A/Y411F)β_3 was specific to NS, we also examined the effect of etomidate (a non-

4   steroidal GABA$_A$R PAM) on muscimol affinity. Etomidate enhanced [^{3}H]muscimol affinity in both the WT

5   and α_1(N408A/Y411F)β_3 receptors, indicating that the effect of these mutations are specific to NS action

6   (Figure 6–figure supplement 1C-D).

7

8   ***3β5αP increases desensitization through binding to α_1 and β_3 intrasubunit sites.***

9   To further explore the relationship between desensitization and enhancement of [^{3}H]muscimol binding,

10   we examined the consequences of mutations to these sites on physiological measurements of desensitization

11   induced by NS. Again, these experiments were performed with 3β5αP because it is the endogenous 3β-OH

12   NS and because of limited quantities of KK148. Desensitization was quantified by defining the baseline

13   steady-state current at 1 mM GABA as 100% and measuring percent reduction of the steady-state current

14   elicited by a NS (Figure 8A). 3β5αP reduced the steady-state current (i.e. enhanced desensitization) by 23.0

15   ± 2.8% (% of desensitization: mean ± SEM, n = 5, Figure 8A). Mutations in the α_1 and β_3 intrasubunit sites

16   [i.e. α_1(N408A/Y411F)β_3 and $\alpha_1\beta_3$(Y284F), respectively] prevented 3β5αP-enhanced desensitization by

17   ~67% (Figure 8B), whereas mutation in the β(+)–α(-) intersubunit site [α_1(Q242L)β_3] was without effect

18   (Figure 8C). Receptors with mutations in both the α_1 and β_3 intrasubunit sites

19   [α_1(N408A/Y411F)β_3(Y284F)] showed less NS-enhancement of desensitization than receptors with

20   mutations in either of the intrasubunit sites alone, indicating that both intrasubunit sites contribute to the

21   desensitizing effect (Figure 8C). Whereas the desensitizing effect of 3β5αP is completely eliminated by the

22   V2'S mutation α_1(V256S)β_3, it is not completely eliminated by combined mutations of all three binding

23   sites [α_1(Q242L/N408A/Y411F)β_3(Y284F)] (Figure 8C). This suggests either that the effects of the

24   mutations are incomplete or there are additional unidentified NS binding sites contributing to

25   desensitization. Since mutations of the α_1 and β_3 intrasubunit sites also disrupt 3β5αP-enhancement of

26   [^{3}H]muscimol binding (Figure 6C), we conclude that 3β5αP binding to these intrasubunit sites stabilizes

1   the desensitized state of the $GABA_AR$ and thus enhances [3H]muscimol binding. Furthermore, KK148

2   increased $GABA_AR$ desensitization (% of desensitization = 27.2 ± 6.0: mean $\pm$ SEM, $n = 3$, Figure 2A) and

3   the $\alpha_1(V256S)\beta_3$ mutation abolished the effect (% of desensitization = 0, $n = 1$). These observations support

4   the idea that binding of certain NS analogues to α_1 and β_3 intrasubunit sites, increases $GABA_AR$

5   desensitization. In contrast, KK150 showed a very small effect on desensitization (% of desensitization =

6   2.1 ± 0.7: mean $\pm$ SEM, $n = 5$, Figure 2B), consistent with the small increase in [3H]muscimol binding by

7   KK150 (Figure 1E).

8

9   ***The effects of 3α5αP binding to intrasubunit sites on desensitization.***

10   3α5αP binds to all three of the NS binding sites on $\alpha_1\beta_3$ $GABA_AR$, and mutations in all three sites reduce

11   3α5αP enhancement of [3H]muscimol binding (Figure 6B). This suggests the possibility that activation by

12   3α5αP (mediated primarily by the $\beta_3(+)$–$\alpha_1(-)$ intersubunit site) masks a desensitizing effect mediated

13   through the β_3 and/or α_1 intrasubunit binding sites. To determine whether intrasubunit binding sites mediate

14   increased desensitization by 3α5αP, we examined the effect of 3α5αP on steady-state currents in receptors

15   with mutations in the α_1 or β_3 intrasubunit site. In these experiments, P_{open} was maximized by activating

16   receptors with 1 mM GABA co-applied with 40 µM pentobarbital (PB) (52) prior to application of 3α5αP;

17   this was necessary because several of the mutated receptors had a P_{open} << 1.0 in response to 1 mM GABA

18   alone. Mutations in the intrasubunit sites were prepared with a background $\alpha_1(Q242L)\beta_3$ mutation to remove

19   3α5αP activation (11,28,29,53) and focus on the effects of 3α5αP on the equilibrium between the open and

20   desensitized states.

21

22   3α5αP produced a small reduction in steady-state current in $\alpha_1(Q242L)\beta_3$ receptors with mutations in

23   neither of the intrasubunit sites (Figure 9A). This inhibitory effect was eliminated by $\alpha_1(V256S)\beta_3$,

24   indicating that it was due to receptor desensitization (Figure 9D). In receptors with combined mutations in

25   the intersubunit and α_1 intrasubunit sites [i.e. $\alpha_1(Q242L/N408A/Y411F)\beta_3$], 3α5αP significantly inhibited

26   the steady-state current (Figure 9B), an effect that was markedly reduced by mutations in the β_3 intrasubunit

15

1   site [α_1(Q242L)β_3(Y284F)] (Figure 9C). These data suggest that 3α5αP exerts a desensitizing effect by

2   binding to the β_3 intrasubunit site and that 3α5αP binding to the α_1 intrasubunit site does not promote

3   desensitization (Figure 9D). Notably, 3α5αP exerted only a modest inhibitory effect in α_1(Q242L)β_3

4   receptors in which occupancy of the β_3 intrasubunit site should promote inhibition. This may be due to a

5   counterbalancing action at the α_1 intrasubunit site, where 3α5αP binding contributes more to receptor

6   activation as demonstrated by our previous observation that mutations in the α_1 intrasubunit site

7   significantly reduce 3α5αP potentiation of GABA-elicited currents (11). These results suggest that in

8   addition to activation, 3α5αP enhances receptor desensitization. Enhanced desensitization by the PAM-NS

9   3α5αP (54) and 3α5α-THDOC (55,56) has been observed in prior studies supporting the current finding

10   with 3α5αP.

1   **DISCUSSION**

2   In this study we examined how site-specific binding to the three identified NS sites on $\alpha_1\beta_3$ GABA$_A$R

3   (11) contributes to the PAM vs. NAM activity of epimeric 3-OH NS. We found that the PAM-NS 3α5αP,

4   but not the NAM-NS 3β5αP, binds to the canonical β_3(+)–α_1(-) intersubunit site that mediates receptor

5   potentiation, explaining the absence of 3β5αP PAM activity. In contrast, 3β5αP binds to intrasubunit sites

6   in the α_1 and β_3 subunits, promoting receptor desensitization. Binding to the intrasubunit sites provides a

7   mechanistic explanation for the NAM effects of 3β5αP (14). 3α5αP also binds to the β_3 intrasubunit site

8   explaining the previously described desensitizing effect of the PAM-NS 3α5αP (54) and 3α5α-THDOC

9   (55,56). Two synthetic NS with diazirine moieties at C3 (KK148 and KK150) were used to identify NS

10   binding sites and shown to bind to the intersubunit as well as both intrasubunit sites. Neither of these ligands

11   potentiated agonist-activated GABA$_A$R currents, reinforcing the importance of the 3α-OH group and its

12   interaction with α_1Q242 in PAM actions. KK148 is an efficacious desensitizing agent, acting through the

13   α_1 and β_3 intrasubunit NS binding sites. KK150, the 17α-epimer of KK148, binds to all three NS binding

14   sites, but neither activates nor desensitizes GABA$_A$Rs, suggesting a potential chemical scaffold for a general

15   NS antagonist. Collectively, these data show that differential occupancy of and efficacy at three discrete NS

16   binding sites determines whether a NS ligand has PAM, NAM, or potentially NS antagonist activity on

17   GABA$_A$Rs.

18

19   The observation that 3β5αP and KK148 enhance orthosteric ligand binding but do not potentiate GABA-

20   elicited currents first suggested that these NAM-NS selectively stabilize a desensitized conformation of the

21   receptor (n.b. there may be multiple desensitized conformations of the receptor, possibly including NS-

22   specific desensitized states, and our data does not address the specific conformations stabilized by NAM-

23   NS. Strictly, our data indicate that the steroids stabilize a non-conducting state that has high affinity to the

24   orthosteric agonist muscimol.) Chang and colleagues have shown that orthosteric ligand affinity (muscimol

25   or GABA) is greater in desensitized and activated (open) GABA$_A$Rs than in resting (closed) receptors, with

26   estimated GABA K$_D$ values of 78.5 μM, 120 nM and 40 nM for the resting, activated and desensitized

1   $\alpha_1\beta_2\gamma_2$ receptors respectively (37). Our experimental and modeling data demonstrate that NAM-NS such as

2   3β5αP or KK148 enhance orthosteric ligand binding by increasing the population of receptors in a

3   desensitized state. It is, however, unclear if 3β5αP or KK148 can promote transition of resting receptors

4   directly to a desensitized state, thus bypassing channel opening. We propose that in the presence of low

5   concentrations of orthosteric agonists (as in the [^{3}H]muscimol binding assays), there is a slow shift of

6   receptors from resting through activated to a desensitized state with minimal change in the population of

7   receptors in the activated state. The slow time course of accumulation of desensitized receptors is illustrated

8   by experiments in which 10 μM 3β5αP is added to membranes that have been fully equilibrated with a low

9   concentration (3 nM) of [^{3}H]muscimol and binding is measured as a function of time. Enhancement of

10 [^{3}H]muscimol binding by 10 μM 3β5αP is slow, with a time constant of 4 min at 4 °C ($\tau = 3.97 \pm 0.15$ min:

11 mean ± SEM, $n = 4$, Supplementary file 1). In contrast, when $\alpha_1\beta_3$ GABA$_A$Rs are exposed to long pulses of

12 a high concentration of GABA, KK148- and 3β5αP-induced desensitization is rapid (Figures 2A and 2C),

13 since in these conditions almost all of the receptors are either in an open or desensitized conformation and

14 desensitization is not slowed by the transition from resting to open state (57). Thus, the slow enhancement

15 of [^{3}H]muscimol binding by 3β5αP (Supplementary file 1) is likely rate-limited by the transition of

16 receptors to activated then to desensitized states at 3 nM muscimol rather than by 3β5αP binding. These

17 time course experiments are most consistent with a model in which receptors preferentially progress from

18 the resting to active to desensitized states, which are then stabilized by the NAM-NS.

19

20 The selective binding of 3β5αP to a subset of identified NS binding sites provides an explanation for its

21 NAM activity. 3β5αP stabilizes desensitized receptors by binding to the α_1 and β_3 intrasubunit sites, but

22 does not activate the receptor because it does not bind to the intersubunit site. This site-selective binding is

23 unexpected for several reasons. First, docking and free energy perturbation calculations in a prior study

24 predicted that epi-pregnanolone (3β5βP) binds to the intersubunit site in a similar orientation and with free

25 energies of binding that are equivalent to pregnanolone (3α5βP) (23). The modeling suggested that 3β5βP

26 does not form a hydrogen bond with αQ242, a possible explanation for its lack of efficacy (23). Our docking

1   studies also show similar binding energies and orientations of 3β5αP and 3α5αP binding in the β$_3$(+)–α$_1$(-)

2   intersubunit site (Supplementary file 2). We have also shown that binding affinity or docking scores of NS

3   binding to the intersubunit site is not significantly affected by mutations (α$_1$Q242L, α$_1$Q242W, α$_1$W246L)

4   that eliminate NS activation, although binding orientation is altered (28). These data indicate that NS

5   binding in the intersubunit site is tolerant to significant changes in critical residues and NS ligand structure,

6   and are consistent with our findings that NS analogues, such as KK148 and KK150, can bind to the

7   intersubunit site but have no effect on activation (Figures 1 and 4). Thus, the peculiar lack of 3β5αP binding

8   to the intersubunit site suggests that either: (1) details in the structure of the intersubunit site in the open

9   conformation that explain the absence of 3β5αP binding are not apparent in current high-resolution

10 structures or; (2) 3β5αP does not bind for other reasons. One plausible explanation is that 3β5αP, like

11 cholesterol, has low chemical activity in the membrane and does not achieve sufficiently available

12 concentration to bind in this site (58). This explanation would require that the chemical activity of 3β5αP

13 differs between the inner and outer leaflets of a plasma membrane since 3β5αP binds to the intrasubunit

14 sites.

15

16   The functional analysis of mutations in each of the three NS binding sites demonstrates that the

17 activating and desensitizing effects of NS result from occupancy of distinct sites. In particular, binding of

18 certain NS (3β5αP, KK148) to α$_1$ and β$_3$ intrasubunit sites modulates the open-desensitized equilibrium.

19 Interestingly, lipid binding to intrasubunit pockets in bacterial pLGICs analogous to the α$_1$ and β$_3$

20 intrasubunit sites in GABA$_A$R, also modulates receptor desensitization; docosahexaenoic acid binding to

21 an intrasubunit site in GLIC (59) and phosphatidylglycerol in ELIC (60) increase and decrease agonist-

22 induced desensitization, respectively. The combined results of mutational analyses and binding data

23 demonstrate that the effects of various NS analogues are also a consequence of their efficacy at each of the

24 sites they occupy. For example, KK148 and KK150 occupy the intersubunit site (Figure 4C), but do not

25 activate GABA$_A$R currents (Figures 1C-D), and KK150 occupies both intrasubunit sites (Figure 4B and

26 Figure 4–figure supplement 1) but does not desensitize the receptor (Figure 2B).

1

2   To explain the effects of the 3-substituted NS analogues, we propose a model in which NS-selective

3   binding at three distinct binding sites on the $GABA_AR$ preferentially stabilizes specific states (resting, open,

4   desensitized) of the receptor (Figure 10). Orthosteric agonist (GABA or muscimol) binding shifts the

5   equilibrium towards high-affinity states (open and desensitized). $3\alpha5\alpha P$ allosterically stabilizes the open

6   state through binding to the β_3–α_1 intersubunit and α_1 intrasubunit sites and stabilizes the desensitized state

7   through the β_3 intrasubunit site (Figure 10A). In contrast, $3\beta5\alpha P$ preferentially stabilizes the desensitized

8   state through binding to both intrasubunit sites (Figure 10B). KK148, like $3\beta5\alpha P$, stabilizes the desensitized

9   state by binding to the intrasubunit sites (Figure 10C). KK148 also binds to the intersubunit site, presumably

10   with no state-dependence, since it is neither an agonist nor an inverse-agonist (Figures 1C and 10C). KK150,

11   which neither activates nor desensitizes $GABA_ARs$ and is not an inverse agonist, binds to all three sites,

12   again presumably with no-state dependence (Figures 1D and 10D). This model predicts that KK148 should

13   act as a competitive antagonist to PAM-NS at the intersubunit site. Indeed, KK148 reduces $3\alpha5\alpha P$

14   potentiation of GABA-elicited currents by about 24% (Supplementary file 3). The model also predicts that

15   KK150 should be a competitive NS antagonist at all three binding sites. Consistent with this prediction,

16   KK150 weakly antagonizes $3\alpha5\alpha P$ potentiation of GABA-elicited currents (12%, Supplementary file 3)

17   and antagonizes $3\alpha5\alpha P$ and KK148 enhancement of [^{3}H]muscimol binding (Figure 7). The modest

18   antagonism of $3\alpha5\alpha P$ potentiation observed with KK148 and KK150 is likely the result of these ligands

19   having lower binding affinity than the 3-OH NS.

20

21   The site-specific model of NS action (Figure 10) has significant implications for the synaptic

22   mechanisms of PAM-NS action. At a synapse, $GABA_ARs$ are transiently exposed to high (mM)

23   concentrations of GABA leading to a channel P_{open} approaching one (61,62). GABA is quickly cleared from

24   the synapse leading to rapid deactivation with minimal desensitization (57,63). In the presence of a PAM-

25   NS, deactivation is slowed, resulting in a prolongation of the inhibitory postsynaptic current (IPSC) and

1   increased inhibitory current (18,55,64,65). This effect is largely attributable to stabilization of the open

2   state, presumably by binding to the intersubunit and α_1 intrasubunit binding sites. A second effect has been

3   observed in which the PAM-NS $3\alpha5\alpha$P (54) and $3\alpha5\alpha$-THDOC (55) prolong the slow component of

4   GABA$_A$R desensitization and slow recovery from desensitization. This results in increased late channel

5   openings (55,57) and IPSC prolongation (64,65). When the frequency of synaptic firing is rapid, the

6   desensitizing effect of NS may also contribute to frequency-dependent reduction in IPSC amplitude (55,66).

7   The desensitizing effect of $3\alpha5\alpha$P is predominantly mediated by binding at the β_3 intrasubunit site. The

8   balance between stabilization of the open and desensitized channels should be determined by the relative

9   occupancies for the intersubunit site of the active receptor and the β_3 intrasubunit site of the desensitized

10   receptor. Computational docking of $3\alpha5\alpha$P to these sites indicates modest differences in affinity between

11   the sites with a rank order affinity of: intersubunit > α_1 intrasubunit > β_3 intrasubunit sites (Supplementary

12   file 2) (11). Mutational analysis of the effects of NS on enhancement of [^{3}H]muscimol binding also indicates

13   that $3\alpha5\alpha$P has a lower affinity to the β_3 intrasubunit site (Figure 6B, Table 1). Thus binding to the β_3

14   intrasubunit site may serve as a negative feedback mechanism preventing excessive PAM-NS effects on

15   synaptic currents.

16

17   In summary, this study describes a unique NS pharmacology in which different NS analogues selectively

18   bind to subsets of three sites on the $\alpha_1\beta_3$ GABA$_A$R, with each analogue exhibiting state-dependent binding

19   at a given site. The combination of site-selectivity and state-dependence of binding determines whether a

20   NS analogue is a PAM, a NAM or an antagonist of NS action at the GABA$_A$R. It seems likely that other

21   GABA$_A$R subunit isoforms and heteropentameric subunit combinations will reveal additional NS binding

22   sites with distinct affinity and state-dependence for various analogues. The identification of potent agonists

23   and antagonists for each of these sites will provide tools for understanding the biological effects of

24   endogenous neurosteroids and potentially for the development of precision neurosteroid therapeutics.

25

26

1 **MATERIALS AND METHODS**

2 *Construct design*

3   The human α_1 and β_3 subunits were subcloned into pcDNA3 for molecular manipulations and cRNA

4 synthesis. Using QuikChange mutagenesis (Agilent Technologies, Santa Clara, CA), a FLAG tag was first

5 added to the α_1 subunit then an octa-histidine tag was added to generate the following His-FLAG tag tandem

6 (QPSLHHHHHHHHDYKDDDDKDEL), inserted between the 4th and 5th residues of the mature peptide.

7 The α_1 and β_3 subunits were then transferred into the pcDNA4/TO and pcDNA5/TO vectors (Thermo Fisher

8 Scientific), respectively, for tetracycline inducible expression. Point mutations were generated using the

9 QuikChange site-directed mutagenesis kit and the coding region fully sequenced prior to use. The cDNAs

10 were linearized with Xba I (NEB Labs, Ipswich, MA), and the cRNAs were generated using T7 mMessage

11 mMachine (Ambion, Austin, TX).

12

13 *Cell culture and generation of stable cell line*

14   Cell culture was performed as described in previous reports (11). The tetracycline inducible cell line T-

15 REx^{TM}-HEK293 (Thermo Fisher Scientific) was cultured under the following conditions: cells were

16 maintained in DMEM/F-12 50/50 medium containing 10% fetal bovine serum (tetracycline-free, Takara,

17 Mountain View, CA), penicillin (100 units/ml), streptomycin (100 g/ml), and blasticidin (2 µg/ml) at 37 °C

18 in a humidified atmosphere containing 5% CO_2. Cells were passaged twice each week, maintaining

19 subconfluent cultures. Stably transfected cells were cultured as above with the addition of hygromycin (50

20 µg/ml) and zeocin (20 µg/ml). A stable cell line was generated by transfecting T-REx^{TM}-HEK293 cells with

21 human α_1-8xHis-FLAG pcDNA4/TO and human β_3 pcDNA5/TO, in a 150 mm culture dish, using the

22 Effectene transfection reagent (Qiagen). Two days after transfection, selection of stably transfected cells

23 was performed with hygromycin and zeocin until distinct colonies appeared. Medium was exchanged

24 several times each week to maintain antibiotic selection. Individual clones were selected from the dish and

25 transferred to 24-well plates for expansion of each clone selected. When the cells grew sufficiently, about

26 50% confluency, they were split into two other plates, one for a surface ELISA against the FLAG epitope

1   and a second for protein assay, to normalize surface expression to cell number. The best eight clones were

2   selected for expansion into 150 mm dishes, followed by [^{3}H]muscimol binding to examine the receptor

3   density. Once the best expressing clone was determined, the highest expressing cells of that clone were

4   selected through fluorescence activated cell sorting.

5

6   ***Membrane protein preparation***

7   Stably transfected cells were plated into dishes. After reaching 50% confluency, GABA receptors were

8   expressed by inducing cells with 1 μg/ml of doxycycline with the addition of 5 mM sodium butyrate. Cells

9   were harvested 48 to 72 hours after induction. HEK cells, after induction, grown to 100% confluency were

10   harvested and washed with 10 mM potassium phosphate, 100 mM potassium chloride (pH 7.5) plus protease

11   inhibitors (Sigma) two times. The cells were collected by centrifugation at 1,000 g at 4 °C for 5 min. The

12   cells were homogenized with a glass mortar and a Teflon pestle for ten strokes on ice. The pellet containing

13   the membrane proteins was collected after centrifugation at 20,000 g at 4 °C for 45 min and resuspended

14   in a buffer containing 10 mM potassium phosphate, 100 mM potassium chloride (pH 7.5). The protein

15   concentration was determined with micro-BCA protein assay and stored at -80 °C.

16

17   ***Photolabeling and purification of α$_1$β$_3$ GABA$_A$R***

18   The syntheses of neurosteroid photolabeling reagents (KK148, KK150, KK200, KK123) are detailed in

19   previous reports (33,36). For all the photolabeling experiments, 10-20 mg of HEK cell membrane proteins

20   (about 300 pmol [^{3}H]muscimol binding) were thawed and resuspended in buffer containing 10 mM

21   potassium phosphate, 100 mM potassium chloride (pH 7.5) and 1 mM GABA at a final concentration of

22   1.25 mg/ml. For the photolabeling competition experiments, 3 μM KK200 or KK123 in the presence of 30

23   μM competitor (3α5αP, KK148, KK150, and 3β5αP) or the same volume of ethanol was added to the

24   membrane proteins and incubated on ice for 1 h. The samples were then irradiated in a quartz cuvette for 5

25   min, by using a photoreactor emitting light at > 320 nm. The membrane proteins were then collected by

26   centrifugation at 20,000 g at 4 °C for 45 min. The photolabeled membrane proteins were resuspended in

1   lysis buffer containing 1% *n*-dodecyl-β-D-maltoside (DDM), 0.25% cholesteryl hemisuccinate (CHS), 50

2   mM Tris (pH 7.5), 150 mM NaCl, 2 mM $CaCl_2$, 5 mM KCl, 5 mM $MgCl_2$, 1 mM EDTA, 10% glycerol at

3   a final concentration of 1 mg/ml. The membrane protein suspension was homogenized using a glass mortar

4   and a Teflon pestle and incubated at 4 °C overnight. The protein lysate was centrifuged at 20,000 g at 4 °C

5   for 45 min and supernatant was incubated with 0.5 ml anti-FLAG agarose (Sigma) at 4 °C for 2 h. The anti-

6   FLAG agarose was then transferred to an empty column, followed by washing with 20 ml washing buffer

7   (50 mM triethylammonium bicarbonate and 0.05% DDM). The $GABA_A$Rs were eluted with aliquots of 200

8   µg/ml FLAG tag peptide and 100 µg/ml 3X FLAG (ApexBio) in the washing buffer. The pooled eluates (9

9   ml) containing $GABA_A$Rs were concentrated to 100 µl using 100 kDa cut-off centrifugal filters.

10

11   ***Tryptic middle-down MS analysis***

12   The purified $α_1β_3$ $GABA_A$R (100 µl) was reduced with 5 mM tris(2-carboxyethyl)phosphine for 1 h,

13   alkylated with 5 mM *N*-ethylmaleimide (NEM) for 1 h, and quenched with 5 mM dithiothreitol (DTT) for

14   15 min. These three steps were done at RT. Samples were then digested with 8 µg of trypsin for 7 days at

15   4 °C to obtain maximal recovery of TMD peptides. Next, the digestion was terminated by adding formic

16   acid in a final concentration of 1%, followed directly by LC-MS analysis on an Orbitrap Elite mass

17   spectrometer. 20 µl samples were injected into a home-packed PLRP-S (Agilent) column (10 cm x 75 µm,

18   300 Å), separated with a 145 min gradient from 10 to 90% acetonitrile, and introduced to the mass

19   spectrometer at 800 nl/min with a nanospray source. MS acquisition was set as a MS1 Orbitrap scan

20   (resolution of 60,000) followed by top 20 MS2 Orbitrap scans (resolution of 15,000) using data-dependent

21   acquisition, and exclusion of singly charged precursors. Fragmentation was performed using high-energy

22   dissociation with normalized energy of 35%. Analysis of data sets was performed using Xcalibur (Thermo

23   Fisher Scientific) to manually search for TM1, TM2, TM3 or TM4 tryptic peptides with or without

24   neurosteroid photolabeling modifications. Photolabeling efficiency was estimated by generating extracted

25   chromatograms of unlabeled and labeled peptides, determining the area under the curve, and calculating

26   the abundance of labeled peptide/(unlabeled + labeled peptide). Analysis of statistical significance

1   comparing the photolabeling efficiency of KK200 and KK123 for $\alpha_1\beta_3$ GABA$_A$R was determined using

2   one-way ANOVA with *post hoc* Bonferroni correction and paired *t*-test, respectively (GraphPad Prism 6).

3   MS2 spectra of photolabeled TMD peptides were analyzed by manual assignment of fragment ions with

4   and without photolabeling modification. Fragment ions were accepted based on the presence of a

5   monoisotopic mass within 20 ppm mass accuracy. In addition to manual analysis, PEAKS (Bioinformatics

6   Solutions Inc.) database searches were performed for data sets of photolabeled $\alpha_1\beta_3$ GABA$_A$R. Search

7   parameters were set for a precursor mass accuracy of 20 ppm, fragment ion accuracy of 0.1 Da, up to 3

8   missed cleavages on either end of the peptide, false discovery rate of 0.1%, and variable modifications of

9   methionine oxidation, cysteine alkylation with NEM and DTT, and NS analogue photolabeling reagents on

10   any amino acid.

11

12   ***Radioligand binding assays***

13   [^{3}H]muscimol binding assays were performed using a previously described method (11). HEK cell

14   membrane proteins (100 μg/ml final concentration) were incubated with 3 nM [^{3}H]muscimol (30 Ci/mmol;

15   PerkinElmer Life Sciences), neurosteroid (3 nM–30 μM) or etomidate (30 nM–200 μM) in different

16   concentrations, binding buffer (10 mM potassium phosphate, 100 mM potassium chloride, pH 7.5), in a

17   total volume of 1 ml. Assay tubes were incubated for 1 h on ice in the dark. Nonspecific binding was

18   determined by binding in the presence of 1 mM GABA. Membranes were collected on Whatman/GF-C

19   glass filter papers using a Brandel cell harvester (Gaithersburg, MD). To perform [^{3}H]muscimol binding

20   isotherms, 100 μg/ml aliquots of membrane protein were incubated with 0.3 nM–1 μM [^{3}H]muscimol, with

21   specific activity reduced to 2 Ci/mmol, for 1 h on ice in the dark. The membranes were collected on

22   Whatman/GF-B glass filter paper using a vacuum manifold. For the [^{3}H]muscimol binding competition,

23   neurosteroids in the presence of competitors (0.3 μM 3α5αP or 3 μM KK148 vs. 30 μM KK150) or the

24   same volume of dimethyl sulfoxide (DMSO) were added to the membrane proteins and incubated with 3

25   nM [^{3}H]muscimol on ice for 1 h. Time courses of neurosteroid [^{3}H]muscimol binding enhancement were

26   examined by adding 10 μM of neurosteroids (3α5αP, 3β5αP) to membranes that had been fully equilibrated

1   with 3 nM [^{3}H]muscimol for 1 h on ice and binding was measured as a function of time at 1, 3, 10, 30, 60

2   min. The membranes were collected on Whatman/GF-B glass filter papers using vacuum manifold.

3   Radioactivity bound to the filters was measured by liquid scintillation spectrometry using Bio-Safe II

4   (Research Products International Corporation).

5

6   *Radioligand binding to intact cells*

7   HEK cells were harvested by gently washing dishes with buffer containing 10 mM sodium phosphate

8   (pH 7.5), 150 mM sodium chloride twice. The cells were collected by centrifugation at 500 g at 4 °C for 5

9   min, and resuspended in isotonic (10 mM sodium phosphate, 150 mM sodium chloride, pH 7.5) or

10   hypotonic (10 mM sodium phosphate, pH 7.5) buffer to prepare two different conditions for radioligand

11   binding to intact cells [isotonic buffer for cell surface receptors; hypotonic buffer for total receptors (cell

12   surface receptors + intracellular receptors)]. The cells were incubated on ice for 2 h, after which the sodium

13   chloride concentration was adjusted to be isotonic before the radioligand binding procedure. HEK cells

14   were aliquoted to assay tubes (20 samples/150 mm dish) in a total volume of 1 ml, and incubated with 3

15   nM [^{3}H]muscimol and 10 μM KK148 for 1 h on ice in the dark. Nonspecific binding was determined by

16   binding in the presence of 1 mM GABA. The membranes were collected on Whatman/GF-B glass filter

17   papers using vacuum manifold. Radioactivity bound to the filters was measured by liquid scintillation

18   spectrometry using Bio-Safe II.

19

20   *Receptor expression in Xenopus laevis oocytes and electrophysiological recordings*

21   The wild-type and mutant $\alpha_1\beta_3$ GABA$_A$R were expressed in oocytes from the African clawed frog

22   (*Xenopus laevis*). Frogs were purchased from Xenopus 1 (Dexter, MI), and housed and cared for in a

23   Washington University Animal Care Facility under the supervision of the Washington University Division

24   of Comparative Medicine. Harvesting of oocytes was conducted under the Guide for the Care and Use of

25   Laboratory Animals as adopted and promulgated by the National Institutes of Health. The animal protocol

26   (No. 20180191) was approved by the Animal Studies Committee of Washington University in St. Louis.

1   The oocytes were injected with a total of 12 ng cRNA. The ratio of cRNAs was 5:1 ratio (α_1:β_3) to minimize

2   the expression of β_3 homomeric receptors. Following injection, the oocytes were incubated in ND96 (96

3   mM NaCl, 2 mM KCl, 1.8 mM CaCl$_2$, 1 mM MgCl$_2$, 5 mM HEPES; pH 7.4) with supplements (2.5 mM

4   Na pyruvate, 100 U/ml penicillin, 100 μg/ml streptomycin and 50 μg/ml gentamycin) at 16 °C for 2 days

5   prior to conducting electrophysiological recordings. The electrophysiological recordings were conducted

6   at room temperature using standard two-electrode voltage clamp. The oocytes were clamped at -60 mV.

7   The chamber (RC-1Z, Warner Instruments, Hamden, CT) was perfused with ND96 at 5-8 ml/min. Solutions

8   were gravity-applied from 30 ml glass syringes with glass luer slips via Teflon tubing. The current responses

9   were amplified with an OC-725C amplifier (Warner Instruments, Hamden, CT), digitized with a Digidata

10   1200 series digitizer (Molecular Devices), and stored using pClamp (Molecular Devices). Current traces

11   were analyzed with Clampfit (Molecular Devices). The stock solution of GABA was made in ND96 at 500

12   mM, stored in aliquots at -20 °C, and diluted on the day of experiment. The stock solution of muscimol was

13   made at 20 mM in ND96 and stored at 4 °C. The steroids were dissolved in DMSO at 10-20 mM and stored

14   at room temperature.

15

16   ***Electrophysiological data analysis and simulations***

17   The raw amplitudes of the current traces were converted to units of open probability through comparison

18   to the peak response to 1 mM GABA + 50 μM propofol, that was considered to have a peak P_{open}

19   indistinguishable from 1 (11). The level of constitutive activity in the absence of any applied agonist was

20   considered negligible and not included in this calculation. The converted current traces were analyzed in

21   the framework of the three-state Resting-Open-Desensitized activation model (44,45). The model enables

22   analysis and prediction of peak responses using four parameters that characterize the extent of constitutive

23   activity (termed L; L = Resting/Open), affinity of the resting receptor to agonist (K_C), affinity of the open

24   receptor to agonist (K_O), and the number of agonist binding sites (N). Analysis and prediction of steady-

25   state responses requires an additional parameter, termed Q, that describes the equilibrium between open

26   and desensitized receptors (Q = Open/Desensitized).

28

1   The P_{open} of the peak response is expressed as:

2

$$P_{open,peak} = \frac{1}{1 + L\Gamma}$$

3

4

5   and the P_{open} of the steady-state response as:

6

$$P_{open,steady-state} = \frac{1}{1 + \dfrac{1}{Q} + L\Gamma}$$

7

8

9

10   where

11

$$\Gamma = \left[\frac{(1 + [X]/K_C)}{(1 + [X]/K_O)} \right]^N$$

12

13

14

15   [X] is the concentration of agonist present, and other terms are as described above. In practice, the value

16   of $L\Gamma$ was calculated using the experimentally-determined P_{open} of the peak response, and then used as a

17   fixed value in estimating Q from $P_{open,steady-state}$.

18   The $P_{desensitized}$ was calculated using:

19

$$P_{desensitized} = \frac{1}{1 + Q + QL\Gamma}$$

20

21

22

23   The effect of 3β5αP on 1 mM GABA-elicited steady-state current was expressed through a change in

24   the value of Q. The modified Q (termed Q*) was then used to predict changes in P_{open} and $P_{desensitized}$ at low

25   [GABA].

26

1   *Docking simulations*

2   A docking template of the $\alpha_1\beta_3$ GABA$_A$R was developed using the crystal structure of the human β_3

3   homopentamer (PDB ID: 4COF) (67). In this structure, the cytoplasmic loop was replaced with the

4   sequence SQPARAA (68). The pentamer subunits were organized as A α_1, B β_3, C α_1, D β_3, E β_3. The α_1

5   sequence was aligned to the β_3 sequence using the program MUSCLE (69). The pentameric alignment was

6   then used as input for the program Modeller (70), using 4COF as the template; a total of 25 models were

7   generated. The best model as evaluated by the DOPE score (71) was then submitted to the H++ server

8   (http://biophysics.cs.vt.edu) to determine charges and optimize hydrogen bonding. The optimized structure

9   was then submitted to the PPM server (https://opm.phar.umich.edu/ppm_server) for orientation into a lipid

10   membrane. The correctly oriented receptor was then submitted to the CHARMM-GUI Membrane Builder

11   server (http://www.charmm-gui.org) to build the fully solvated, membrane bound system oriented into a 1-

12   palmitoyl-2-oleoyl-sn-glycero-3-phosphatidylcholine (POPC) bilayer. The system was fully solvated with

13   40715 TIP3 water molecules and ionic strength set to 0.15 M KCl. The NAMD input files produced by

14   CHARMM-GUI (72) use a seven-step process of gradually loosening constraints in the simulation prior to

15   production runs. A 100 ns molecular dynamics trajectory was then obtained using the CHARMM36 force

16   field and NAMD (72). The resulting trajectory was then processed using the utility mdtraj (73), to extract

17   a snapshot of the receptor at each nanosecond of time frame. These structures were then mutually aligned

18   by fitting the alpha carbons, providing a set of 100 mutually aligned structures used for docking studies.

19   The docking was performed using AutoDock Vina (74) on each of the 100 snapshots in order to capture

20   receptor flexibility. $3\alpha5\alpha$P and $3\beta5\alpha$P were prepared by converting the sdf file from PubChem into a PDB

21   file using Open Babel (75), and Gasteiger charges and free torsion angles were determined by AutoDock

22   Tools. Docking grid boxes were built for the β_3-α_1 intersubunit, and the α_1 and β_3 intrasubunit sites with

23   dimensions of $15 \times 15 \times 15$ Ångströms encompassing each binding pocket. Docking was limited to an

24   energy range of 3 kcal from the best docking pose and was limited to a total of 20 unique poses. The docking

25   results for a given site could result in a maximum of 2,000 unique poses (20 poses $\times$ 100 receptor structures);

1   these were then clustered geometrically using the program DIVCF (76). The resulting clusters were ranked

2   by Vina score and cluster size, and then visually analyzed.

3

TABLE AND FIGURES

$3\alpha5\alpha P$	EC_{50} (μM)	Hill slope	E_{max} (% of control)	n
WT$\alpha_1\beta_3$	0.24 ± 0.04	1.10 ± 0.14	374.1 ± 11.1	6
α_1(Q242L)β_3	**2.66 ± 0.51	1.16 ± 0.37	**159.8 ± 10.9	6
α_1(N408A/Y411F)β_3	**2.30 ± 0.48	0.87 ± 0.44	**146.0 ± 9.3	6
$\alpha_1\beta_3$(Y284F)	0.19 ± 0.04	0.87 ± 0.16	342.3 ± 13.9	6
α_1(Q242L/N408A/Y411F)β_3	-	-	**105.9 ± 7.3	6
$3\beta5\alpha P$				
WT$\alpha_1\beta_3$	0.25 ± 0.08	0.84 ± 0.23	195.1 ± 6.7	3
α_1(Q242L)β_3	0.27 ± 0.09	0.77 ± 0.21	204.3 ± 4.5	3
α_1(N408A/Y411F)β_3	0.61 ± 0.26	2.25 ± 0.92	**124.3 ± 2.6	3
$\alpha_1\beta_3$(Y284F)	-	-	**148.6 ± 4.9	3
KK148				
WT$\alpha_1\beta_3$	2.40 ± 0.36	1.36 ± 0.16	431.0 ± 19.5	6
α_1(Q242L)β_3	2.20 ± 0.31	1.24 ± 0.12	434.5 ± 5.6	6
α_1(N408A/Y411F)β_3	1.63 ± 0.53	0.73 ± 0.23	**161.7 ± 3.5	6
α_1(V227W)β_3	1.73 ± 0.68	0.76 ± 0.31	**209.2 ± 7.4	6
$\alpha_1\beta_3$(Y284F)	1.79 ± 0.44	1.35 ± 0.13	**357.2 ± 8.1	6
Etomidate				
WT$\alpha_1\beta_3$	7.24 ± 1.18	1.07 ± 0.17	331.1 ± 9.9	6
α_1(Q242L)β_3	7.50 ± 0.95	1.35 ± 0.20	**277.8 ± 10.9	6
α_1(N408A/Y411F)β_3	9.14 ± 2.20	1.07 ± 0.26	**268.2 ± 5.9	6
$\alpha_1\beta_3$(Y284F)	7.71 ± 1.10	0.90 ± 0.11	303.5 ± 5.8	6
$\alpha_1\beta_3$(M286W)	*22.5 ± 6.17	0.50 ± 0.16	**128.6 ± 7.8	6

TABLE 1: **Effects of mutations on neurosteroid modulation of [^{3}H]muscimol binding.** EC_{50}, Hill slope and maximal effect values [E_{max} (% of control): 100% means no effect] for the concentration-response curves in Figures 6B-E. Statistical differences are analyzed using one-way ANOVA with *post hoc* Bonferroni correction (*$P < 0.05$ vs. WT; **$P < 0.01$ vs. WT). Data are presented as mean ± SEM.
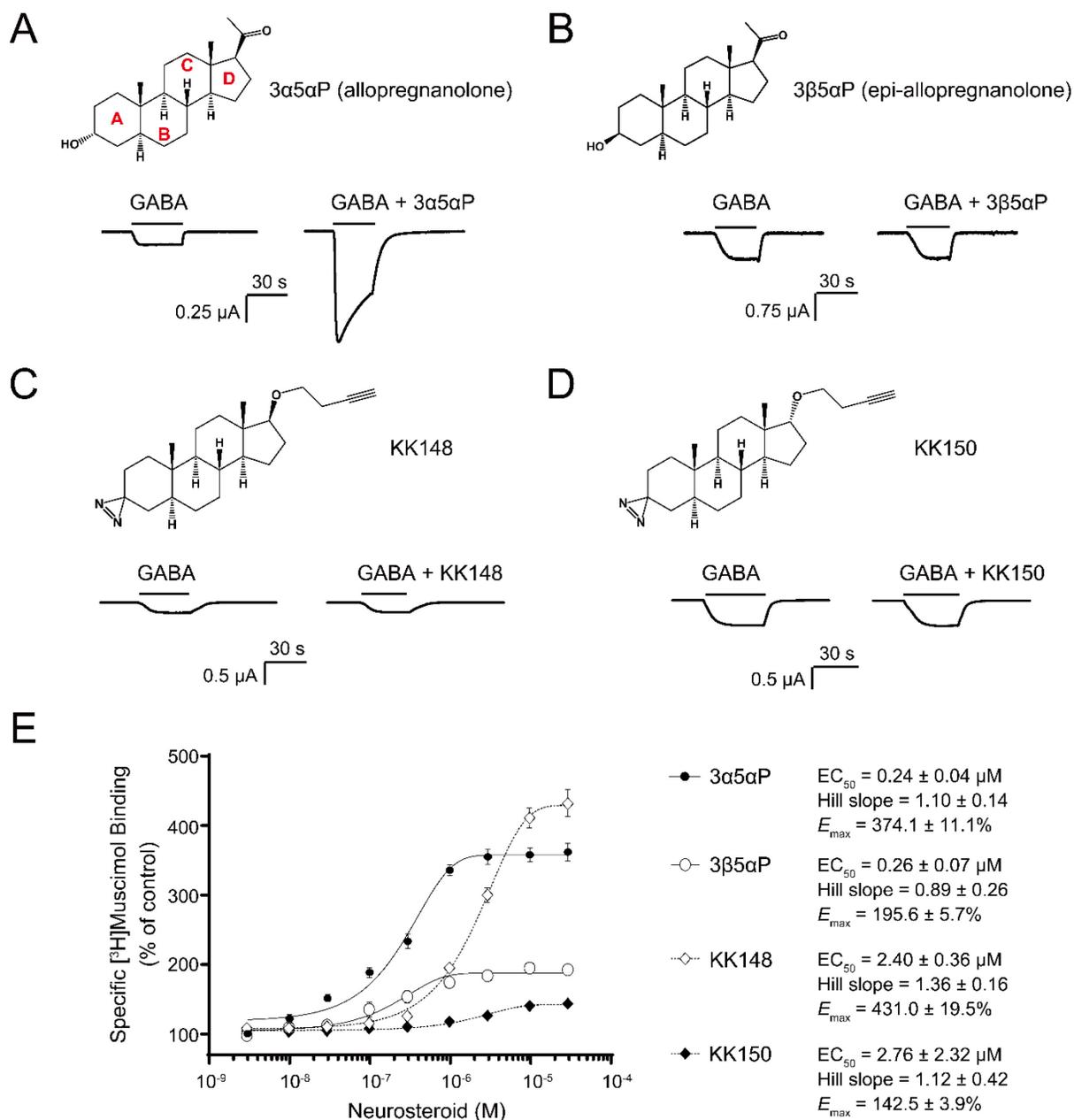
FIGURE 1: **Distinct neurosteroid effects on potentiation of GABA$_A$R currents and modulation of [^{3}H]muscimol binding.** (A) Structure of allopregnanolone (3α5αP) and sample current traces from α$_1$β$_3$ GABA$_A$R activated by 0.3 μM GABA showing potentiation by 10 μM 3α5αP. (B), (C) and (D) Structures of epi-allopregnanolone (3β5αP), neurosteroid analogue photolabeling reagents KK148 and KK150, respectively, and sample current traces from α$_1$β$_3$ GABA$_A$R activated by 0.3 μM GABA showing the absence of potentiation by 10 μM neurosteroids. (E) Concentration-response relationship for neurosteroid modulation of [^{3}H]muscimol binding to α$_1$β$_3$ GABA$_A$R. 3 nM–30 μM neurosteroids modulate [^{3}H]muscimol (3 nM) binding in a concentration-dependent manner. Data points, EC$_{50}$, Hill slope and maximal effect value [E_{max} (% of control): 100% means no effect] are presented as mean ± SEM (n = 6 for 3α5αP and KK148; n = 3 for 3β5αP and KK150).
Figure 1–figure supplement 1: Neurosteroid modulation of muscimol binding to intact cells.

33
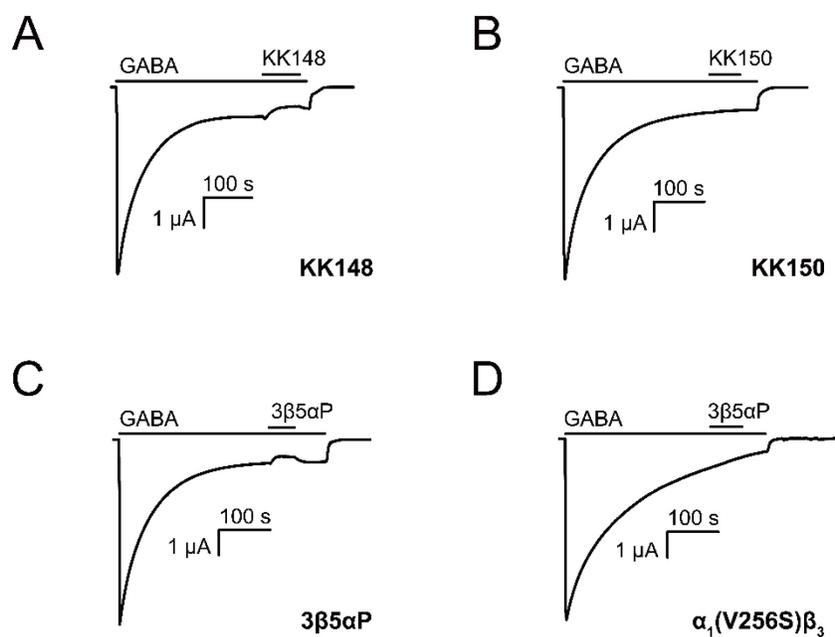
FIGURE 2: **Neurosteroids promote steady-state desensitization of $\alpha_1\beta_3$ GABA$_A$Rs.** Representative traces showing the effects of KK148, KK150 and epi-allopregnanolone (3β5αP) on maximal steady-state GABA-elicited currents. $\alpha_1\beta_3$ GABA$_A$Rs expressed in *Xenopus laevis* oocytes were activated with 1 mM GABA to maximally activate GABA$_A$R current. (A-C) The effect of KK148 (10 μM), KK150 (10 μM) and 3β5αP (3 μM) on steady-state current. (D) The effect of 3β5αP (3 μM) on steady-state current in $\alpha_1\beta_3$ GABA$_A$Rs containing the α_1V256S mutation, known to eliminate NS-induced desensitization. The results show that 3β5αP and KK148 reduce steady-state currents, consistent with enhanced desensitization, whereas KK150 does not. The effect of 3β5αP on steady-state currents is eliminated by the α_1V256S mutation, consistent with 3β5αP enhancing desensitization rather than producing channel block.
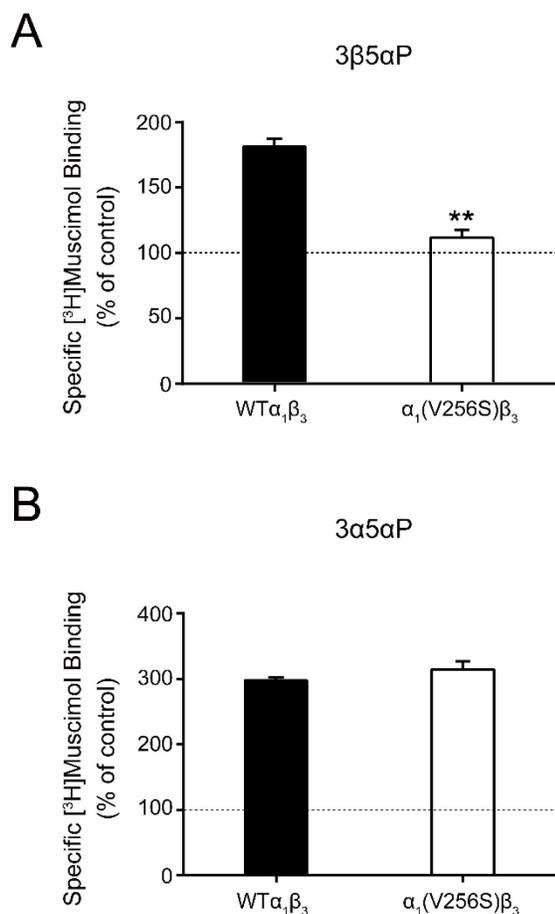
FIGURE 3: **Effect of α_1(V256S)β_3 mutation on neurosteroid enhancement of [^{3}H]muscimol binding.** (A) Enhancement of specific [^{3}H]muscimol (3 nM) binding to $\alpha_1\beta_3$ GABA$_A$R WT by 10 μM epi-allopregnanolone (3β5αP) is absent in α_1(V256S)β_3 GABA$_A$R. (B) Enhancement of [^{3}H]muscimol binding by 10 μM allopregnanolone (3α5αP) is unaffected by the α_1V256S mutation. These data indicate that 3β5αP enhancement of orthosteric ligand binding requires receptor desensitization, whereas 3α5αP does not. ($n = 6$, ± SEM). **$P < 0.01$ vs. WT.
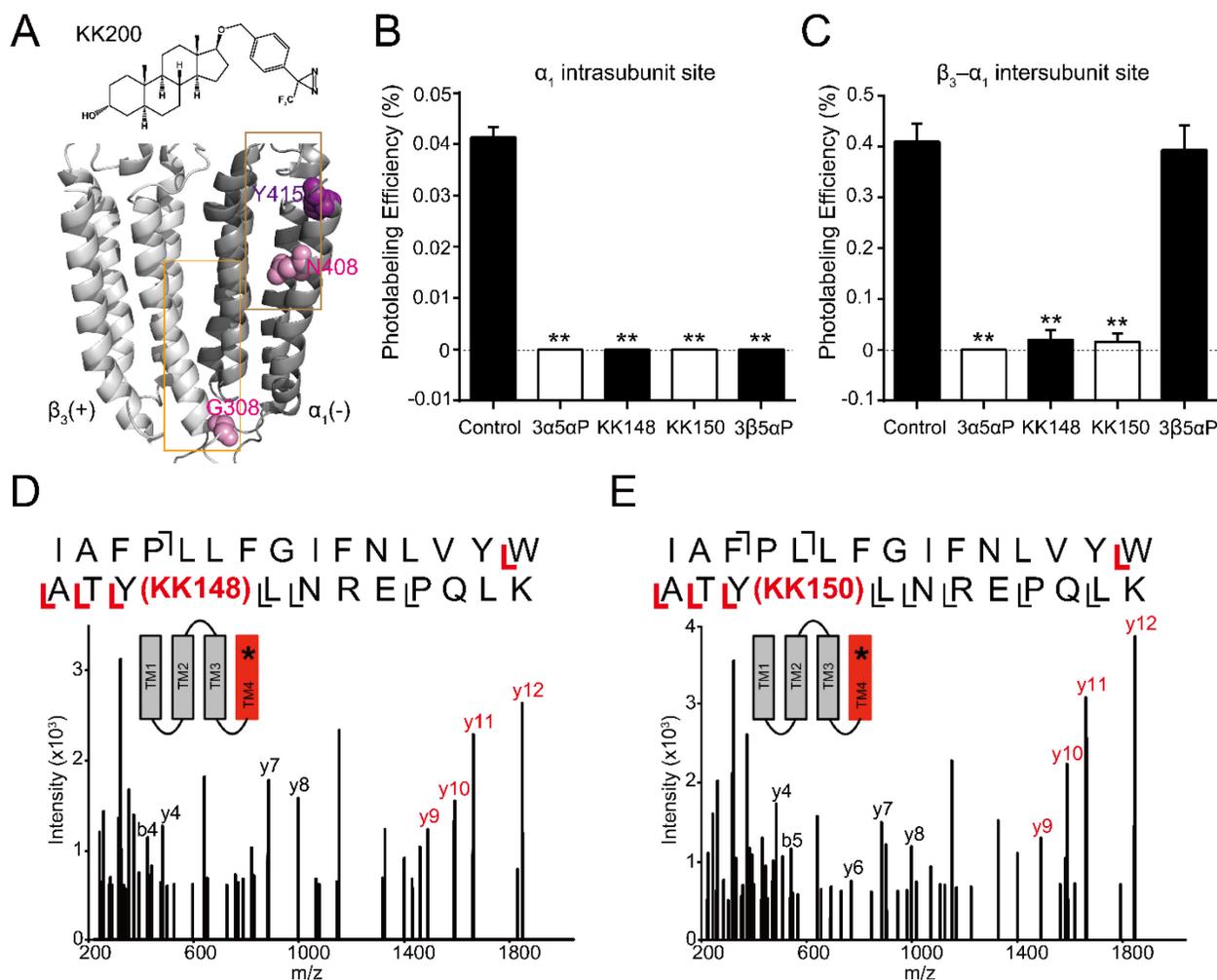
FIGURE 4: **Competitive prevention of neurosteroid photolabeling at an intersubunit and intrasubunit site.** (A) Structures of the neurosteroid photolabeling reagent KK200 and the $\alpha_1\beta_3$ GABA$_A$R-TMDs highlighting the residues G308 in the $\beta_3(+)-\alpha_1(-)$ intersubunit site and N408 in the α_1 intrasubunit site previously identified by KK200 photolabeling in pink. Shown in purple is Y415 in the α_1 intrasubunit site, which is photolabeled by KK148 and KK150. Adjacent $\beta_3(+)$ and $\alpha_1(-)$ subunits are shown and the channel pore is behind the subunits. (B) Photolabeling efficiency of α_1 subunit TM4 (α_1 intrasubunit site) in $\alpha_1\beta_3$ GABA$_A$R by 3 μM KK200 in the absence or presence of 30 μM allopregnanolone (3α5αP), KK148, KK150, and epi-allopregnanolone (3β5αP) ($n = 3$, ± SEM). **$P < 0.01$ vs. control. (C) Same as (B) for β_3 subunit TM3 [$\beta_3(+)-\alpha_1(-)$ intersubunit site, $n = 3$, ± SEM]. (D) HCD fragmentation spectrum of the α_1 subunit TM4 tryptic peptide photolabeled by 30 μM KK148. Red and black indicate fragment ions that do or do not contain KK148, respectively. The schematic highlight in red identifies the TMD being analyzed and the asterisk denotes the approximate location of KK148. (E) Same as (D) photolabeled by 30 μM KK150.

Figure 4–figure supplement 1: Extracted ion chromatograms of labeled and unlabeled β_3 subunit TM4 peptides.

Figure 4–figure supplement 2: Fragmentation spectrum of unlabeled α_1 subunit TM4 peptide.
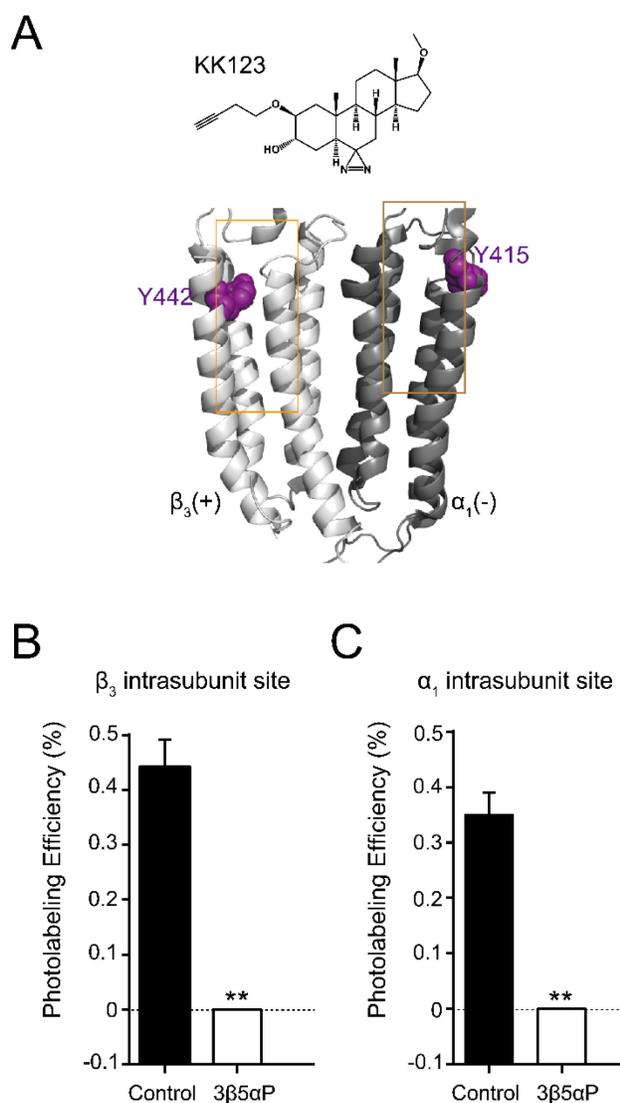
FIGURE 5: **Epi-allopregnanolone prevents neurosteroid photolabeling at the α_1 and β_3 intrasubunit sites.** (A) Structures of the neurosteroid photolabeling reagent KK123 and the $\alpha_1\beta_3$ GABA$_A$R-TMDs highlighting the residues Y442 in the β_3 intrasubunit site and Y415 in the α_1 intrasubunit site previously identified by KK123 photolabeling in purple. Adjacent β_3(+) and α_1(-) subunits are shown and the channel pore is behind the subunits. (B) Photolabeling efficiency of β_3 subunit TM4 (β_3 intrasubunit site) in $\alpha_1\beta_3$ GABA$_A$R by 3 μM KK123 in the absence or presence of 30 μM epi-allopregnanolone (3β5αP) ($n = 3$, $\pm$ SEM). **$P < 0.01$ vs. control. (C) Same as (B) for α_1 subunit TM4 (α_1 intrasubunit site, $n = 3$, $\pm$ SEM).

37
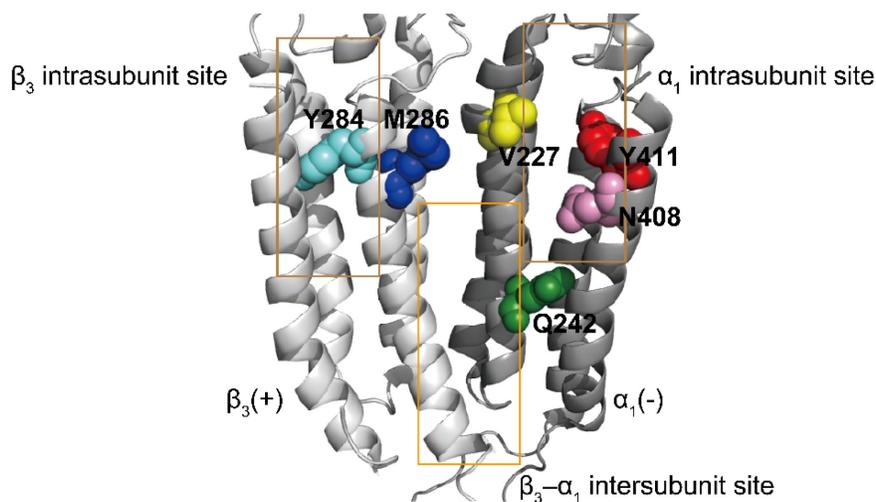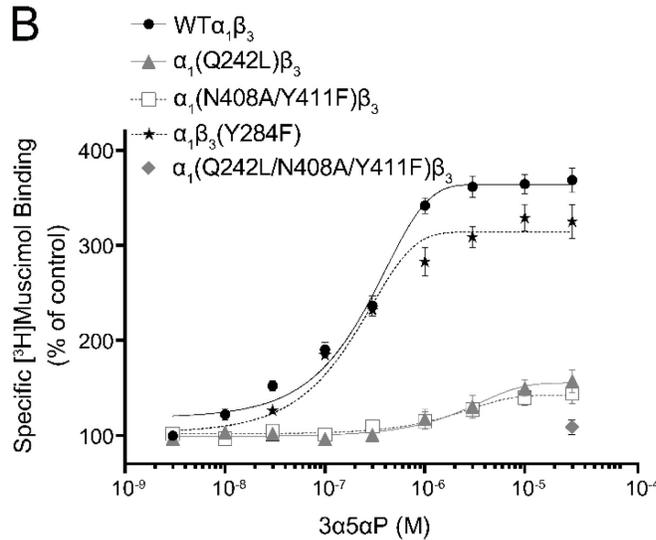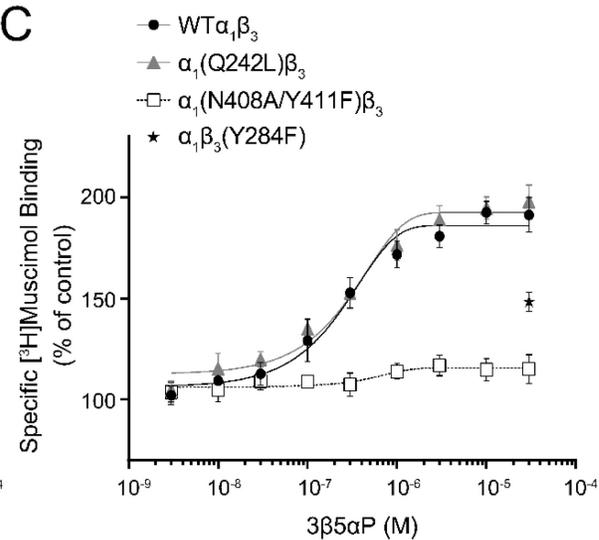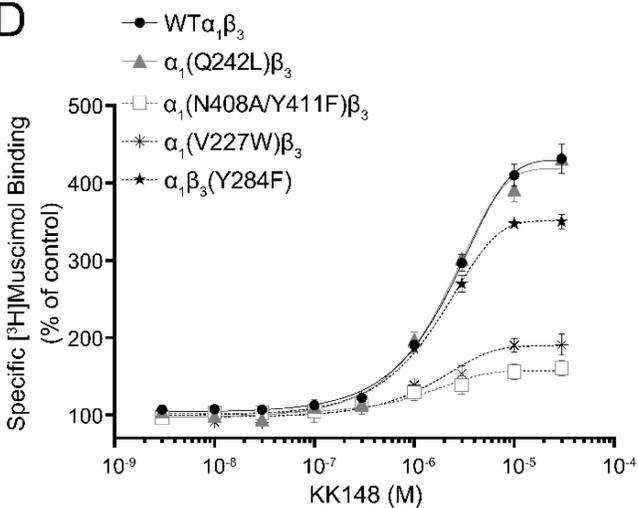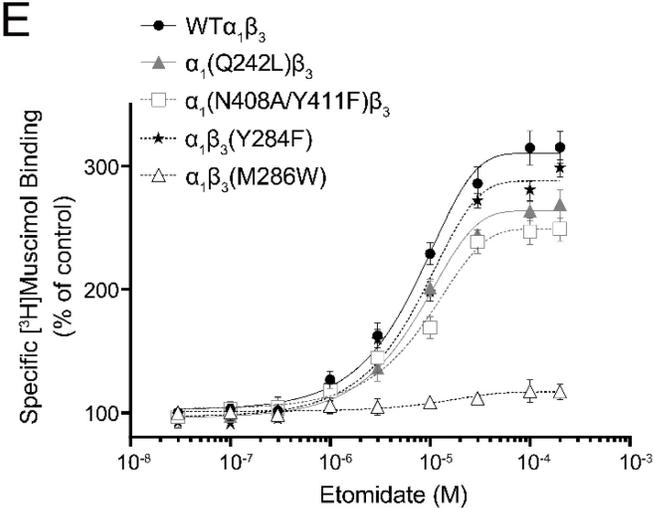
FIGURE 6: **Effect of mutations in $\alpha_1\beta_3$ GABA$_A$R on neurosteroid modulation of [^{3}H]muscimol binding.** (A) Structure of the $\alpha_1\beta_3$ GABA$_A$R-TMD highlighting the residues where mutations were made in putative binding sites for neurosteroids (Q242-green for β_3–α_1 intersubunit site; V227-yellow, N408-pink and Y411-red for α_1 intrasubunit site; Y284-cyan for β_3 intrasubunit site) and M286-blue for etomidate. Adjacent β_3(+) and α_1(-) subunits are shown and the channel pore is behind the subunits. (B) Concentration-response relationship for the effect of 3 nM–30 μM allopregnanolone ($3\alpha5\alpha$P) on [^{3}H]muscimol (3 nM) binding to $\alpha_1\beta_3$ GABA$_A$R WT and indicated mutants. Data points represent mean ± SEM ($n = 6$). (C), (D) and (E) Same as (B) for 3 nM–30 μM epi-allopregnanolone ($3\beta5\alpha$P) ($n = 3$), KK148 ($n = 6$) and 30 nM–200 μM etomidate ($n = 6$), respectively. The data for WT in panels 6B and 6D is a replot of the same data shown in Figure 1E.

Figure 6–figure supplement 1: Neurosteroid effect on [^{3}H]muscimol binding isotherms in $\alpha_1\beta_3$ WT and α_1(N408A/Y411F)β_3 GABA$_A$Rs.

Figure 6–figure supplement 2: Properties of [^{3}H]muscimol saturation binding curves in the $\alpha_1\beta_3$ GABA$_A$R WT and α_1(N408A/Y411F)β_3 mutant.
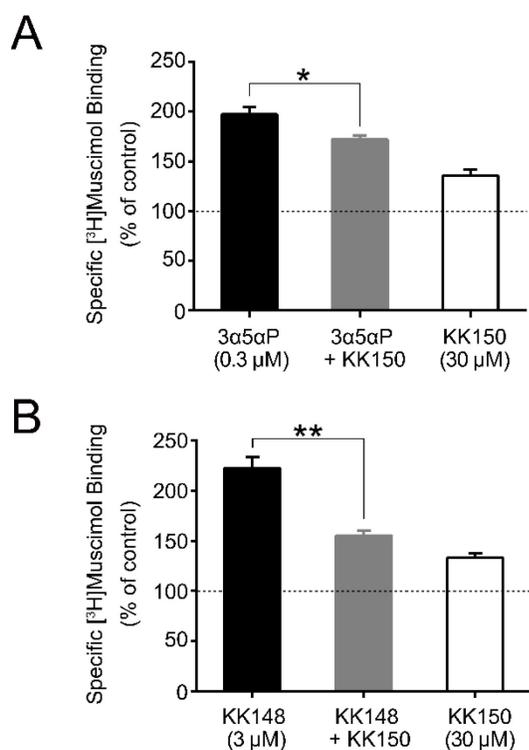
FIGURE 7: **KK150 prevents neurosteroid-induced muscimol binding enhancement.** (A) Enhancement of specific [^{3}H]muscimol (3 nM) binding to $\alpha_1\beta_3$ GABA$_A$R by 0.3 μM allopregnanolone (3α5αP) in the absence (black bar) or presence (grey bar) of 30 μM KK150 and KK150 alone (white bar) ($n = 8$, ± SEM). *$P < 0.05$ vs. 0.3 μM 3α5αP alone. (B) Same as (A) for 3 μM KK148 ($n = 8$, ± SEM). **$P < 0.01$ vs. 3 μM KK148 alone.

40
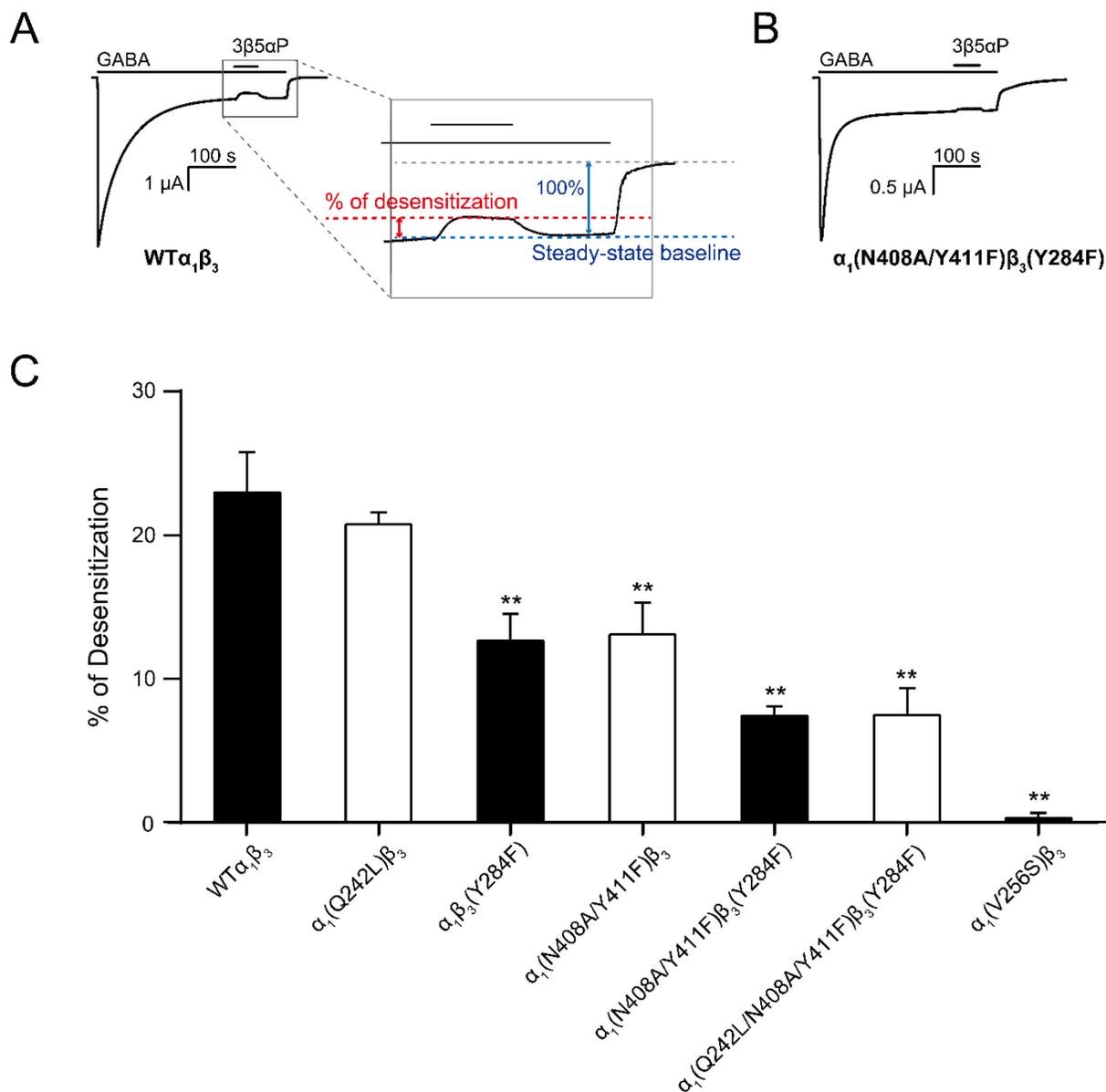
FIGURE 8: **Mutations in intrasubunit sites prevent desensitization by epi-allopregnanolone.** (A) Sample current trace showing the effect of 3 μM epi-allopregnanolone (3β5αP) on $\alpha_1\beta_3$ GABA$_A$R activated by 1 mM GABA. A zoomed-in box shows neurosteroid-induced desensitization of the steady-state GABA current. (B) Same as (A) for α_1(N408A/Y411F)β_3(Y284F) GABA$_A$R. (C) Percent desensitization of the steady-state $\alpha_1\beta_3$ GABA$_A$R currents (WT and mutants) by 3 μM 3β5αP during continuous application of 1 mM GABA. ($n = 5$, ± SEM). **$P < 0.01$ vs. WT.
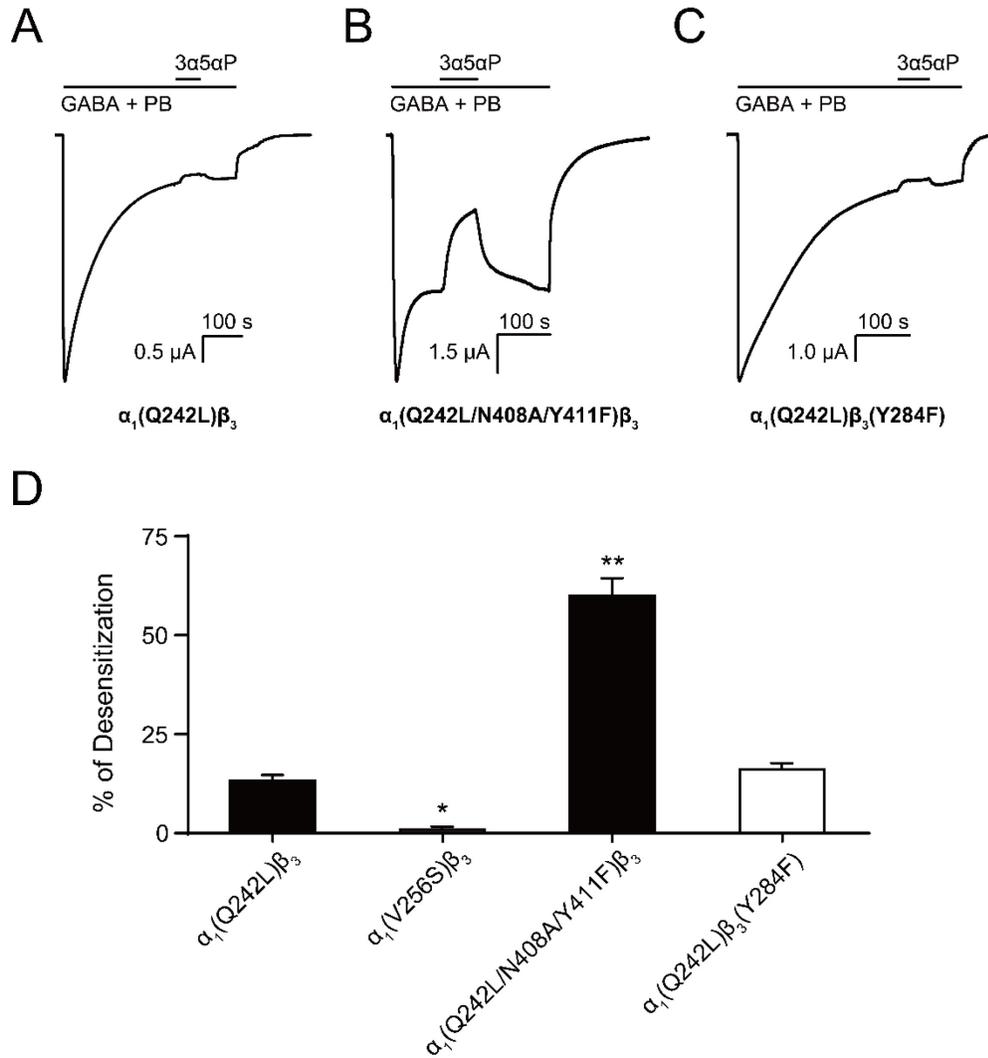
FIGURE 9: **Allopregnanolone desensitizes GABA$_A$R currents via binding to the β$_3$ intrasubunit site.** (A) Sample current trace showing the effect of 3 μM allopregnanolone (3α5αP) on α$_1$(Q242L)β$_3$ GABA$_A$R activated by 1 mM GABA co-applied with 40 μM pentobarbital (PB). (B), (C) Same as (A) for α$_1$(Q242L/N408A/Y411F)β$_3$ GABA$_A$R and α$_1$(Q242L)β$_3$(Y284F) GABA$_A$R, respectively. (D) Percent desensitization of the steady-state currents elicited by 1 mM GABA with 40 μM PB in α$_1$β$_3$ GABA$_A$R with specified mutations [$n = 4$ for α$_1$(V256S)β$_3$; $n = 5$ for others, ± SEM]. *$P < 0.05$; **$P < 0.01$ vs. α$_1$(Q242L)β$_3$, respectively.

43
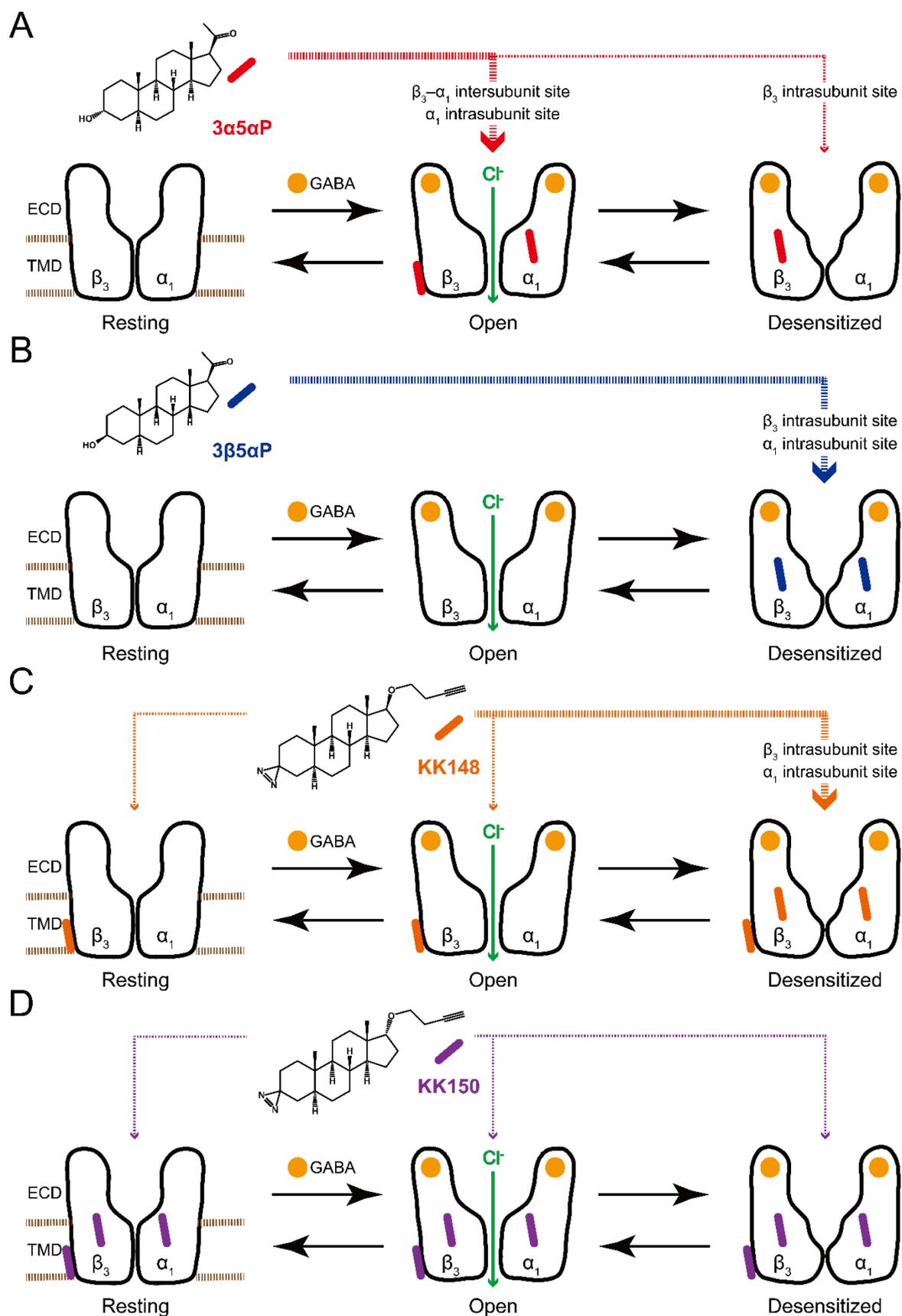
FIGURE 10: **Neurosteroids preferentially stabilize GABA$_A$R in different states.** (A) Model showing three fundamental conformational states that depict the channel function in the GABA$_A$R: a resting state; an open state; and a desensitized state. Agonist (GABA: 🟡) binding shifts the equilibrium towards high-affinity states (open and desensitized). Allopregnanolone (3α5αP: ⬭) allosterically stabilizes the high-affinity states (an open state through the β$_3$–α$_1$ intersubunit and the α$_1$ intrasubunit sites; a desensitized state through the β$_3$ intrasubunit site). The width of red arrows indicates relative affinities of 3α5αP for the open or desensitized state of the receptor. (B) Same as (A) for epi-allopregnanolone (3β5αP: ⬭). 3β5αP stabilizes a desensitized state through the β$_3$ and α$_1$ intrasubunit sites. (C) Same as (A) for KK148 (⬭). KK148 allosterically stabilizes a desensitized state through the β$_3$ and α$_1$ intrasubunit sites, and equally stabilizes all three states of the receptor through the β$_3$–α$_1$ intersubunit site. The width of orange arrows indicates relative affinities of KK148 for each state of the receptor. (D) Same as (A) for KK150 (⬭). KK150 equally stabilizes all three states of the receptor through the β$_3$ and α$_1$ intrasubunit sites, and the β$_3$–α$_1$ intersubunit site.

REFERENCES

1. Belelli, D., and Lambert, J. J. (2005) Neurosteroids: endogenous regulators of the GABA(A) receptor. *Nat Rev Neurosci* **6**, 565-575

2. Mitchell, E. A., Herd, M. B., Gunn, B. G., Lambert, J. J., and Belelli, D. (2008) Neurosteroid modulation of GABAA receptors: molecular determinants and significance in health and disease. *Neurochem Int* **52**, 588-595

3. Represa, A., and Ben-Ari, Y. (2005) Trophic actions of GABA on neuronal development. *Trends Neurosci* **28**, 278-283

4. Grobin, A. C., Gizerian, S., Lieberman, J. A., and Morrow, A. L. (2006) Perinatal allopregnanolone influences prefrontal cortex structure, connectivity and behavior in adult rats. *Neuroscience* **138**, 809-819

5. Akk, G., Covey, D. F., Evers, A. S., Steinbach, J. H., Zorumski, C. F., and Mennerick, S. (2007) Mechanisms of neurosteroid interactions with GABA(A) receptors. *Pharmacol Ther* **116**, 35-57

6. Reddy, D. S., and Estes, W. A. (2016) Clinical Potential of Neurosteroids for CNS Disorders. *Trends Pharmacol Sci* **37**, 543-561

7. Kharasch, E. D., and Hollmann, M. W. (2015) Steroid Anesthesia Revisited: Again. *Anesth Analg* **120**, 983-984

8. Gunduz-Bruce, H., Silber, C., Kaul, I., Rothschild, A. J., Riesenberg, R., Sankoh, A. J., Li, H., Lasser, R., Zorumski, C. F., Rubinow, D. R., Paul, S. M., Jonas, J., Doherty, J. J., and Kanes, S. J. (2019) Trial of SAGE-217 in Patients with Major Depressive Disorder. *N Engl J Med* **381**, 903-911

9. Zorumski, C. F., Paul, S. M., Covey, D. F., and Mennerick, S. (2019) Neurosteroids as novel antidepressants and anxiolytics: GABA-A receptors and beyond. *Neurobiol Stress* **11**, 100196

10. Akk, G., Covey, D. F., Evers, A. S., Mennerick, S., Zorumski, C. F., and Steinbach, J. H. (2010) Kinetic and structural determinants for GABA-A receptor potentiation by neuroactive steroids. *Curr Neuropharmacol* **8**, 18-25

11. Chen, Z. W., Bracamontes, J. R., Budelier, M. M., Germann, A. L., Shin, D. J., Kathiresan, K., Qian, M. X., Manion, B., Cheng, W. W. L., Reichert, D. E., Akk, G., Covey, D. F., and Evers, A. S. (2019) Multiple functional neurosteroid binding sites on GABAA receptors. *PLoS Biol* **17**, e3000157

12. Olsen, R. W. (2018) GABAA receptor: Positive and negative allosteric modulators. *Neuropharmacology* **136**, 10-22

13. Akk, G., Bracamontes, J., and Steinbach, J. H. (2001) Pregnenolone sulfate block of GABA(A) receptors: mechanism and involvement of a residue in the M2 region of the alpha subunit. *J Physiol* **532**, 673-684

14. Wang, M., He, Y., Eisenman, L. N., Fields, C., Zeng, C. M., Mathews, J., Benz, A., Fu, T., Zorumski, E., Steinbach, J. H., Covey, D. F., Zorumski, C. F., and Mennerick, S. (2002) 3beta - hydroxypregnane steroids are pregnenolone sulfate-like GABA(A) receptor antagonists. *J Neurosci* **22**, 3366-3375

15. Shen, W., Mennerick, S., Covey, D. F., and Zorumski, C. F. (2000) Pregnenolone sulfate modulates inhibitory synaptic transmission by enhancing GABA(A) receptor desensitization. *J Neurosci* **20**, 3571-3579

16. Lundgren, P., Stromberg, J., Backstrom, T., and Wang, M. (2003) Allopregnanolone-stimulated GABA-mediated chloride ion flux is inhibited by 3beta-hydroxy-5alpha-pregnan-20-one (isoallopregnanolone). *Brain Res* **982**, 45-53

17. Seljeset, S., Bright, D. P., Thomas, P., and Smart, T. G. (2018) Probing GABAA receptors with inhibitory neurosteroids. *Neuropharmacology* **136**, 23-36

18. Harrison, N. L., Majewska, M. D., Harrington, J. W., and Barker, J. L. (1987) Structure-activity relationships for steroid interaction with the gamma-aminobutyric acidA receptor complex. *J Pharmacol Exp Ther* **241**, 346-353

19.   Sigel, E., and Steinmann, M. E. (2012) Structure, function, and modulation of GABA(A) receptors. *J Biol Chem* **287**, 40224-40231

20.   Sieghart, W. (2015) Allosteric modulation of GABAA receptors via multiple drug-binding sites. *Adv Pharmacol* **72**, 53-96

21.   Olsen, R. W., and Sieghart, W. (2008) International Union of Pharmacology. LXX. Subtypes of gamma-aminobutyric acid(A) receptors: classification on the basis of subunit composition, pharmacology, and function. Update. *Pharmacol Rev* **60**, 243-260

22.   Laverty, D., Desai, R., Uchanski, T., Masiulis, S., Stec, W. J., Malinauskas, T., Zivanov, J., Pardon, E., Steyaert, J., Miller, K. W., and Aricescu, A. R. (2019) Cryo-EM structure of the human alpha1beta3gamma2 GABAA receptor in a lipid bilayer. *Nature* **565**, 516-520

23.   Miller, P. S., Scott, S., Masiulis, S., De Colibus, L., Pardon, E., Steyaert, J., and Aricescu, A. R. (2017) Structural basis for GABA$_A$ receptor potentiation by neurosteroids. *Nat Struct Mol Biol* **24**, 986-992

24.   Laverty, D., Thomas, P., Field, M., Andersen, O. J., Gold, M. G., Biggin, P. C., Gielen, M., and Smart, T. G. (2017) Crystal structures of a GABA$_A$-receptor chimera reveal new endogenous neurosteroid-binding sites. *Nat Struct Mol Biol* **24**, 977-985

25.   Hosie, A. M., Wilkins, M. E., da Silva, H. M., and Smart, T. G. (2006) Endogenous neurosteroids regulate GABA$_A$ receptors through two discrete transmembrane sites. *Nature* **444**, 486-489

26.   Hosie, A. M., Clarke, L., da Silva, H., and Smart, T. G. (2009) Conserved site for neurosteroid modulation of GABA A receptors. *Neuropharmacology* **56**, 149-154

27.   Chen, Q., Wells, M. M., Arjunan, P., Tillman, T. S., Cohen, A. E., Xu, Y., and Tang, P. (2018) Structural basis of neurosteroid anesthetic action on GABAA receptors. *Nat Commun* **9**, 3972

28.   Sugasawa, Y., Bracamontes, J. R., Krishnan, K., Covey, D. F., Reichert, D. E., Akk, G., Chen, Q., Tang, P., Evers, A. S., and Cheng, W. W. L. (2019) The molecular determinants of neurosteroid binding in the GABA(A) receptor. *J Steroid Biochem Mol Biol* **192**, 105383

29.   Akk, G., Li, P., Bracamontes, J., Reichert, D. E., Covey, D. F., and Steinbach, J. H. (2008) Mutations of the GABA-A receptor alpha1 subunit M1 domain reveal unexpected complexity for modulation by neuroactive steroids. *Mol Pharmacol* **74**, 614-627

30.   Akk, G., Bracamontes, J. R., Covey, D. F., Evers, A., Dao, T., and Steinbach, J. H. (2004) Neuroactive steroids have multiple actions to potentiate GABA$_A$ receptors. *J Physiol* **558**, 59-74

31.   Evers, A. S., Chen, Z. W., Manion, B. D., Han, M., Jiang, X., Darbandi-Tonkabon, R., Kable, T., Bracamontes, J., Zorumski, C. F., Mennerick, S., Steinbach, J. H., and Covey, D. F. (2010) A synthetic 18-norsteroid distinguishes between two neuroactive steroid binding sites on GABA$_A$ receptors. *J Pharmacol Exp Ther* **333**, 404-413

32.   Park-Chung, M., Malayev, A., Purdy, R. H., Gibbs, T. T., and Farb, D. H. (1999) Sulfated and unsulfated steroids modulate gamma-aminobutyric acidA receptor function through distinct sites. *Brain Res* **830**, 72-87

33.   Jiang, X., Shu, H. J., Krishnan, K., Qian, M., Taylor, A. A., Covey, D. F., Zorumski, C. F., and Mennerick, S. (2016) A clickable neurosteroid photolabel reveals selective Golgi compartmentalization with preferential impact on proximal inhibition. *Neuropharmacology* **108**, 193-206

34.   Budelier, M. M., Cheng, W. W. L., Bergdoll, L., Chen, Z. W., Janetka, J. W., Abramson, J., Krishnan, K., Mydock-McGrane, L., Covey, D. F., Whitelegge, J. P., and Evers, A. S. (2017) Photoaffinity labeling with cholesterol analogues precisely maps a cholesterol-binding site in voltage-dependent anion channel-1. *J Biol Chem* **292**, 9294-9304

35.   Budelier, M. M., Cheng, W. W. L., Chen, Z. W., Bracamontes, J. R., Sugasawa, Y., Krishnan, K., Mydock-McGrane, L., Covey, D. F., and Evers, A. S. (2018) Common binding sites for cholesterol and neurosteroids on a pentameric ligand-gated ion channel. *Biochim Biophys Acta Mol Cell Biol Lipids* **1864**, 128-136

36.   Cheng, W. W. L., Chen, Z. W., Bracamontes, J. R., Budelier, M. M., Krishnan, K., Shin, D. J., Wang, C., Jiang, X., Covey, D. F., Akk, G., and Evers, A. S. (2018) Mapping two neurosteroid-

modulatory sites in the prototypic pentameric ligand-gated ion channel GLIC. *J Biol Chem* **293**, 3013-3027

37. Chang, Y., Ghansah, E., Chen, Y., Ye, J., and Weiss, D. S. (2002) Desensitization mechanism of GABA receptors revealed by single oocyte binding and receptor function. *J Neurosci* **22**, 7982-7990

38. Abramian, A. M., Comenencia-Ortiz, E., Modgil, A., Vien, T. N., Nakamura, Y., Moore, Y. E., Maguire, J. L., Terunuma, M., Davies, P. A., and Moss, S. J. (2014) Neurosteroids promote phosphorylation and membrane insertion of extrasynaptic GABA$_A$ receptors. *Proc Natl Acad Sci U S A* **111**, 7132-7137

39. Comenencia-Ortiz, E., Moss, S. J., and Davies, P. A. (2014) Phosphorylation of GABAA receptors influences receptor trafficking and neurosteroid actions. *Psychopharmacology (Berl)* **231**, 3453-3465

40. Smith, S. S., Shen, H., Gong, Q. H., and Zhou, X. (2007) Neurosteroid regulation of GABA(A) receptors: Focus on the alpha4 and delta subunits. *Pharmacol Ther* **116**, 58-76

41. Vauquelin, G., Van Liefde, I., and Swinney, D. C. (2015) Radioligand binding to intact cells as a tool for extended drug screening in a representative physiological context. *Drug Discov Today Technol* **17**, 28-34

42. Bylund, D. B., Deupree, J. D., and Toews, M. L. (2004) Radioligand-binding methods for membrane preparations and intact cells. *Methods Mol Biol* **259**, 1-28

43. Bylund, D. B., and Toews, M. L. (1993) Radioligand binding methods: practical guide and tips. *Am J Physiol* **265**, L421-429

44. Germann, A. L., Pierce, S. R., Burbridge, A. B., Steinbach, J. H., and Akk, G. (2019) Steady-State Activation and Modulation of the Concatemeric alpha 1 beta 2 gamma 2L GABA(A) Receptor. *Molecular Pharmacology* **96**, 320-329

45. Germann, A. L., Pierce, S. R., Senneff, T. C., Burbridge, A. B., Steinbach, J. H., and Akk, G. (2019) Steady-state activation and modulation of the synaptic-type alpha1beta2gamma2L GABAA receptor by combinations of physiological and clinical ligands. *Physiol Rep* **7**, e14230

46. Eaton, M. M., Germann, A. L., Arora, R., Cao, L. Q., Gao, X., Shin, D. J., Wu, A., Chiara, D. C., Cohen, J. B., Steinbach, J. H., Evers, A. S., and Akk, G. (2016) Multiple Non-Equivalent Interfaces Mediate Direct Activation of GABAA Receptors by Propofol. *Curr Neuropharmacol* **14**, 772-780

47. Das, J. (2011) Aliphatic diazirines as photoaffinity probes for proteins: recent developments. *Chem Rev* **111**, 4405-4417

48. Li, G. D., Chiara, D. C., Sawyer, G. W., Husain, S. S., Olsen, R. W., and Cohen, J. B. (2006) Identification of a GABAA receptor anesthetic binding site at subunit interfaces by photolabeling with an etomidate analog. *J Neurosci* **26**, 11599-11605

49. Jayakar, S. S., Zhou, X., Chiara, D. C., Jarava-Barrera, C., Savechenkov, P. Y., Bruzik, K. S., Tortosa, M., Miller, K. W., and Cohen, J. B. (2019) Identifying Drugs that Bind Selectively to Intersubunit General Anesthetic Sites in the alpha1beta3gamma2 GABAAR Transmembrane Domain. *Mol Pharmacol* **95**, 615-628

50. Stewart, D., Desai, R., Cheng, Q., Liu, A., and Forman, S. A. (2008) Tryptophan mutations at azi-etomidate photo-incorporation sites on alpha1 or beta2 subunits enhance GABAA receptor gating and reduce etomidate modulation. *Mol Pharmacol* **74**, 1687-1695

51. Ziemba, A. M., Szabo, A., Pierce, D. W., Haburcak, M., Stern, A. T., Nourmahnad, A., Halpin, E. S., and Forman, S. A. (2018) Alphaxalone Binds in Inner Transmembrane beta+-alpha- Interfaces of alpha1beta3gamma2 gamma-Aminobutyric Acid Type A Receptors. *Anesthesiology* **128**, 338-351

52. Steinbach, J. H., and Akk, G. (2001) Modulation of GABA(A) receptor channel gating by pentobarbital. *J Physiol* **537**, 715-733

53. Bracamontes, J. R., and Steinbach, J. H. (2009) Steroid interaction with a single potentiating site is sufficient to modulate GABA-A receptor function. *Mol Pharmacol* **75**, 973-981

54. Haage, D., and Johansson, S. (1999) Neurosteroid modulation of synaptic and GABA-evoked currents in neurons from the rat medial preoptic nucleus. *J Neurophysiol* **82**, 143-151

55. Zhu, W. J., and Vicini, S. (1997) Neurosteroid prolongs GABAA channel deactivation by altering kinetics of desensitized states. *J Neurosci* **17**, 4022-4031

56. Bianchi, M. T., and Macdonald, R. L. (2003) Neurosteroids shift partial agonist activation of GABA(A) receptor channels from low- to high-efficacy gating patterns. *J Neurosci* **23**, 10934-10943

57. Jones, M. V., and Westbrook, G. L. (1995) Desensitized states prolong GABAA channel responses to brief agonist pulses. *Neuron* **15**, 181-191

58. Lange, Y., and Steck, T. L. (2016) Active membrane cholesterol as a physiological effector. *Chem Phys Lipids* **199**, 74-93

59. Basak, S., Schmandt, N., Gicheru, Y., and Chakrapani, S. (2017) Crystal structure and dynamics of a lipid-induced potential desensitized-state of a pentameric ligand-gated channel. *Elife* **6**

60. Tong, A., Petroff, J. T., 2nd, Hsu, F. F., Schmidpeter, P. A., Nimigean, C. M., Sharp, L., Brannigan, G., and Cheng, W. W. (2019) Direct binding of phosphatidylglycerol at specific sites modulates desensitization of a ligand-gated ion channel. *Elife* **8**

61. Farrant, M., and Nusser, Z. (2005) Variations on an inhibitory theme: phasic and tonic activation of GABA(A) receptors. *Nat Rev Neurosci* **6**, 215-229

62. Feng, H. J., and Forman, S. A. (2018) Comparison of alphabetadelta and alphabetagamma GABAA receptors: Allosteric modulation and identification of subunit arrangement by site-selective general anesthetics. *Pharmacol Res* **133**, 289-300

63. Overstreet, L. S., Jones, M. V., and Westbrook, G. L. (2000) Slow desensitization regulates the availability of synaptic GABA(A) receptors. *J Neurosci* **20**, 7914-7921

64. Harrison, N. L., Vicini, S., and Barker, J. L. (1987) A steroid anesthetic prolongs inhibitory postsynaptic currents in cultured rat hippocampal neurons. *J Neurosci* **7**, 604-609

65. Chakrabarti, S., Qian, M., Krishnan, K., Covey, D. F., Mennerick, S., and Akk, G. (2016) Comparison of Steroid Modulation of Spontaneous Inhibitory Postsynaptic Currents in Cultured Hippocampal Neurons and Steady-State Single-Channel Currents from Heterologously Expressed alpha1beta2gamma2L GABA(A) Receptors. *Mol Pharmacol* **89**, 399-406

66. Jones, M. V., and Westbrook, G. L. (1996) The impact of receptor desensitization on fast synaptic transmission. *Trends Neurosci* **19**, 96-101

67. Miller, P. S., and Aricescu, A. R. (2014) Crystal structure of a human GABA$_A$ receptor. *Nature* **512**, 270-275

68. Jansen, M., Bali, M., and Akabas, M. H. (2008) Modular design of Cys-loop ligand-gated ion channels: functional 5-HT3 and GABA rho1 receptors lacking the large cytoplasmic M3M4 loop. *J Gen Physiol* **131**, 137-146

69. Edgar, R. C. (2004) MUSCLE: a multiple sequence alignment method with reduced time and space complexity. *BMC Bioinformatics* **5**, 113

70. Sali, A., and Blundell, T. L. (1993) Comparative protein modelling by satisfaction of spatial restraints. *J Mol Biol* **234**, 779-815

71. Shen, M. Y., and Sali, A. (2006) Statistical potential for assessment and prediction of protein structures. *Protein Sci* **15**, 2507-2524

72. Lee, J., Cheng, X., Swails, J. M., Yeom, M. S., Eastman, P. K., Lemkul, J. A., Wei, S., Buckner, J., Jeong, J. C., Qi, Y., Jo, S., Pande, V. S., Case, D. A., Brooks, C. L., 3rd, MacKerell, A. D., Jr., Klauda, J. B., and Im, W. (2016) CHARMM-GUI Input Generator for NAMD, GROMACS, AMBER, OpenMM, and CHARMM/OpenMM Simulations Using the CHARMM36 Additive Force Field. *J Chem Theory Comput* **12**, 405-413

73. McGibbon, R. T., Beauchamp, K. A., Harrigan, M. P., Klein, C., Swails, J. M., Hernandez, C. X., Schwantes, C. R., Wang, L. P., Lane, T. J., and Pande, V. S. (2015) MDTraj: A Modern Open Library for the Analysis of Molecular Dynamics Trajectories. *Biophys J* **109**, 1528-1532

48

74. Trott, O., and Olson, A. J. (2010) AutoDock Vina: improving the speed and accuracy of docking with a new scoring function, efficient optimization, and multithreading. *J Comput Chem* **31**, 455-461

75. O'Boyle, N. M., Banck, M., James, C. A., Morley, C., Vandermeersch, T., and Hutchison, G. R. (2011) Open Babel: An open chemical toolbox. *J Cheminform* **3**, 33

76. Meslamani, J. E., Andre, F., and Petitjean, M. (2009) Assessing the Geometric Diversity of Cytochrome P450 Ligand Conformers by Hierarchical Clustering with a Stop Criterion. *J Chem Inf Model* **49**, 330-337

SUPPLEMENTAL MATERIALS

Site-specific effects of neurosteroids on GABA$_A$ receptor activation and desensitization

Yusuke Sugasawa, Wayland W. L. Cheng, John R. Bracamontes, Zi-Wei Chen, Lei Wang,

Allison L. Germann, Spencer R. Pierce, Thomas C. Senneff, Kathiresan Krishnan,

David E. Reichert, Douglas F. Covey, Gustav Akk, Alex S. Evers

FIGURE 1–FIGURE SUPPLEMENT 1

FIGURE 4–FIGURE SUPPLEMENTS 1-2

FIGURE 6–FIGURE SUPPLEMENTS 1-2

SUPPLEMENTARY FILES 1-3
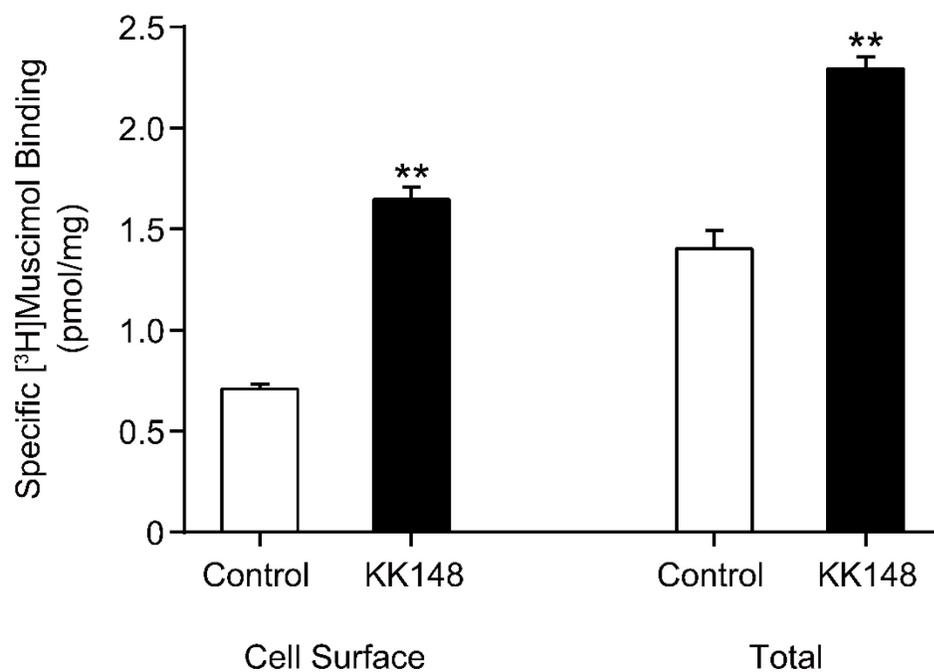
50

FIGURE 1–FIGURE SUPPLEMENT 1: **Neurosteroid modulation of muscimol binding to intact cells.** Enhancement of specific [^{3}H]muscimol (3 nM) binding to $\alpha_1\beta_3$ GABA$_A$Rs on intact HEK cell surfaces (left bars) and total receptors (cell surface receptors + intracellular receptors, right bars) by 10 μM KK148 ($n = 6$, ± SEM). The larger amount of control binding in total vs. cell surface demonstrates the distribution of GABA$_A$R between plasma membrane and intracellular membrane. **$P < 0.01$ vs. control.
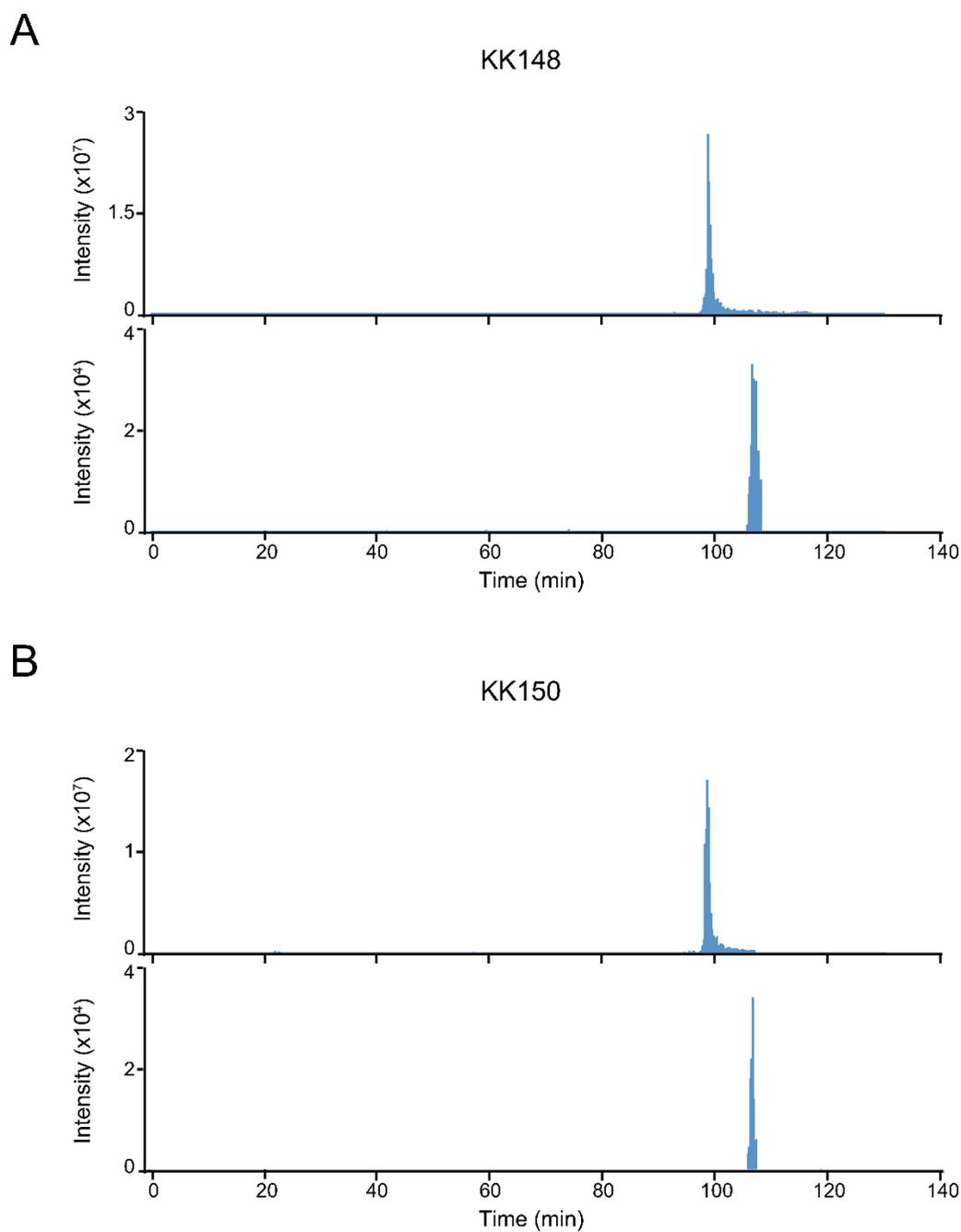
FIGURE 4–FIGURE SUPPLEMENT 1: **Extracted ion chromatograms of labeled and unlabeled β3 subunit TM4 peptides.** (A) Extracted ion chromatogram (XIC) of the β_3 subunit TM4 tryptic peptide in the $\alpha_1\beta_3$ GABA$_A$R. The upper and lower XIC show representative unlabeled β_3 subunit TM4 peptide and the peptide labeled with 30 μM KK148, respectively. (B) Same as (A) for KK150.
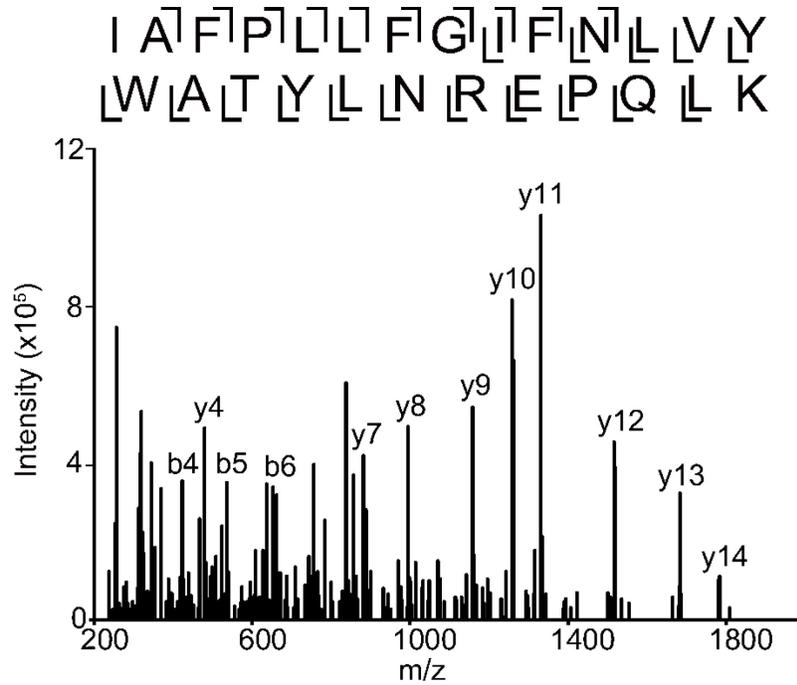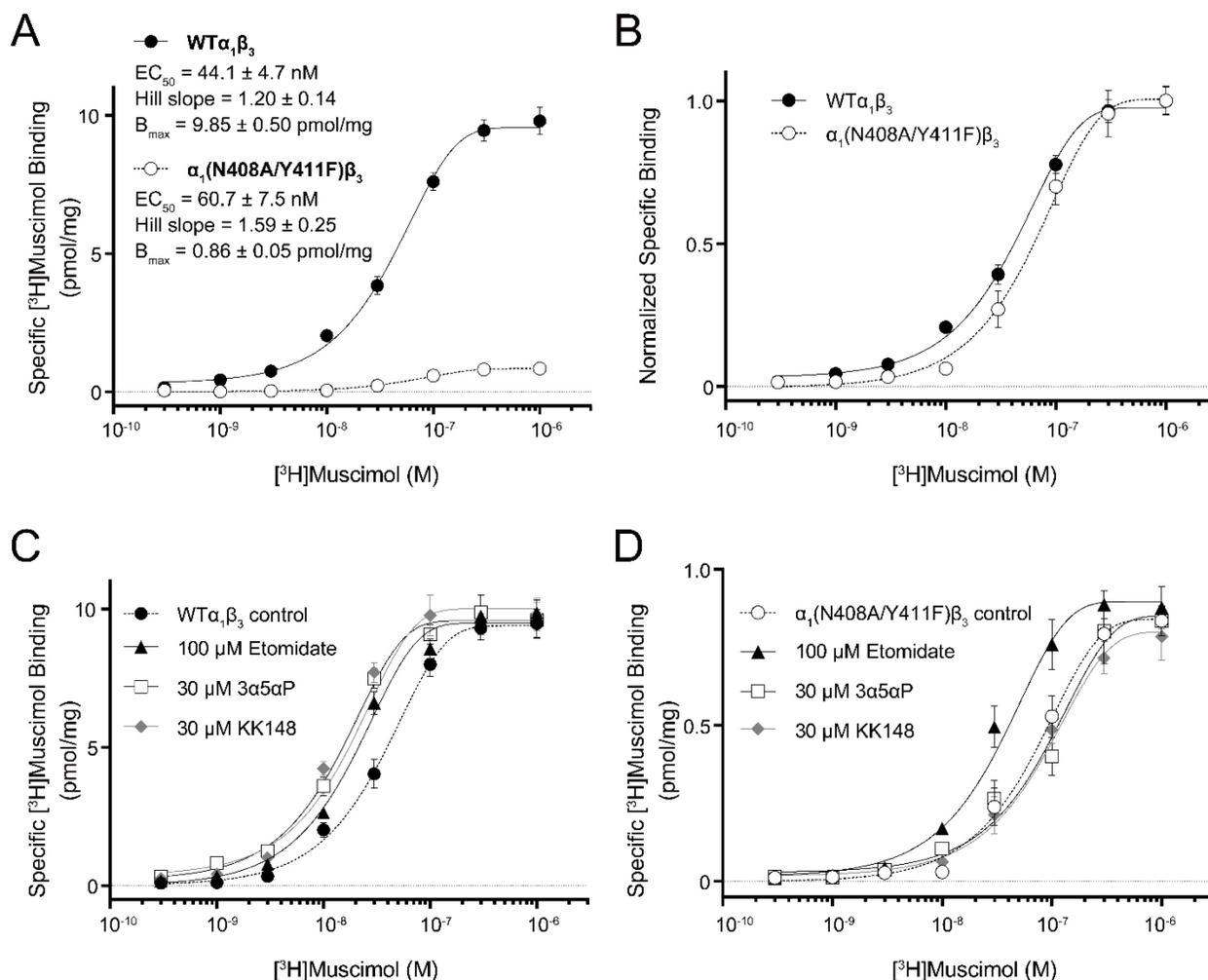
FIGURE 4–FIGURE SUPPLEMENT 2: **Fragmentation spectrum of unlabeled α1 subunit TM4 peptide.** HCD fragmentation spectrum of the α1 subunit TM4 unlabeled tryptic peptide in the α1β3 GABAAR.

FIGURE 6–FIGURE SUPPLEMENT 1: **Neurosteroid effect on [³H]muscimol binding isotherms in α₁β₃ WT and α₁(N408A/Y411F)β₃ GABAₐRs.** (A) [³H]muscimol binding isotherms (0.3 nM–1 μM) for α₁β₃ GABAₐR WT and α₁(N408A/Y411F)β₃ GABAₐR. The EC_{50}, Hill slope and B_{max} are presented as mean ± SEM (n = 3). (B) Normalized curves of specific [³H]muscimol binding shown in (A). (C) Effect of 100 μM etomidate, 30 μM allopregnanolone (3α5αP) and 30 μM KK148 on [³H]muscimol binding isotherms in the α₁β₃ GABAₐR WT. (D) Same as (C) in the α₁(N408A/Y411F)β₃ mutant. Each data point represents mean ± SEM from triplicate experiments.

$WT\alpha_1\beta_3$	EC_{50} (nM)		Hill slope
Control	35.5 ± 4.2		1.32 ± 0.18
Etomidate (100 μM)	19.9 ± 1.6 (*$P = 0.026$ vs. control)		1.43 ± 0.15
3α5αP (30 μM)	15.1 ± 1.6 (*$P = 0.011$ vs. control)		1.57 ± 0.24
KK148 (30 μM)	12.6 ± 1.3 (*$P < 0.01$ vs. control)		1.60 ± 0.24
α_1(N408A/Y411F)β_3			
Control	68.2 ± 12.3		1.41 ± 0.30
Etomidate	27.0 ± 3.9 (*$P = 0.033$ vs. control)		1.45 ± 0.28
3α5αP	98.4 ± 29.6 ($P = 0.399$ vs. control)		1.05 ± 0.28
KK148	72.8 ± 12.8 ($P = 0.808$ vs. control)		1.30 ± 0.25
$WT\alpha_1\beta_3$	Statistical difference between the curves		
Control vs. Etomidate	$F_{7,32} = 3.27$, *$P < 0.01$		
Control vs. 3α5αP	$F_{7,32} = 4.27$, *$P < 0.01$		
Control vs. KK148	$F_{7,32} = 5.96$, *$P < 0.01$		
α_1(N408A/Y411F)β_3			
Control vs. Etomidate	$F_{7,32} = 2.21$, $P = 0.060$		
Control vs. 3α5αP	$F_{7,32} = 0.71$, $P = 0.662$		
Control vs. KK148	$F_{7,32} = 0.29$, $P = 0.952$		

FIGURE 6–FIGURE SUPPLEMENT 2: **Properties of [³H]muscimol saturation binding curves in the $\alpha_1\beta_3$ GABA$_A$R WT and α_1(N408A/Y411F)β_3 mutant.** EC_{50} and Hill slope for the [³H]muscimol saturation binding curves in Figure 6–figure supplement 1C-D. EC_{50} values were compared by unpaired t-test. Statistical differences between the whole curves are analyzed using two-way ANOVA. Data are presented as mean ± SEM ($n = 3$).
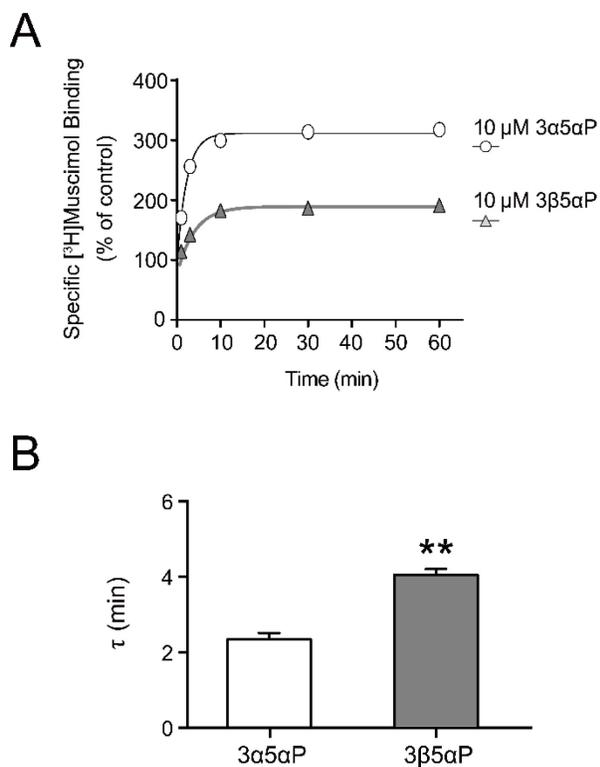
SUPPLEMENTARY FILE 1: **Time course of neurosteroid modulation of muscimol binding.** (A) Time course of [³H]muscimol binding enhancement by 10 µM allopregnanolone (3α5αP) and epi-allopregnanolone (3β5αP). Neurosteroids were added to $\alpha_1\beta_3$ GABA$_A$R membranes that had been fully equilibrated with 3 nM [³H]muscimol and binding was measured as a function of time ($n = 4, \pm$ SEM). (B) Time constants for neurosteroid-induced enhancement of [³H]muscimol binding ($n = 4, \pm$ SEM). **$P < 0.01$ vs. 3α5αP.
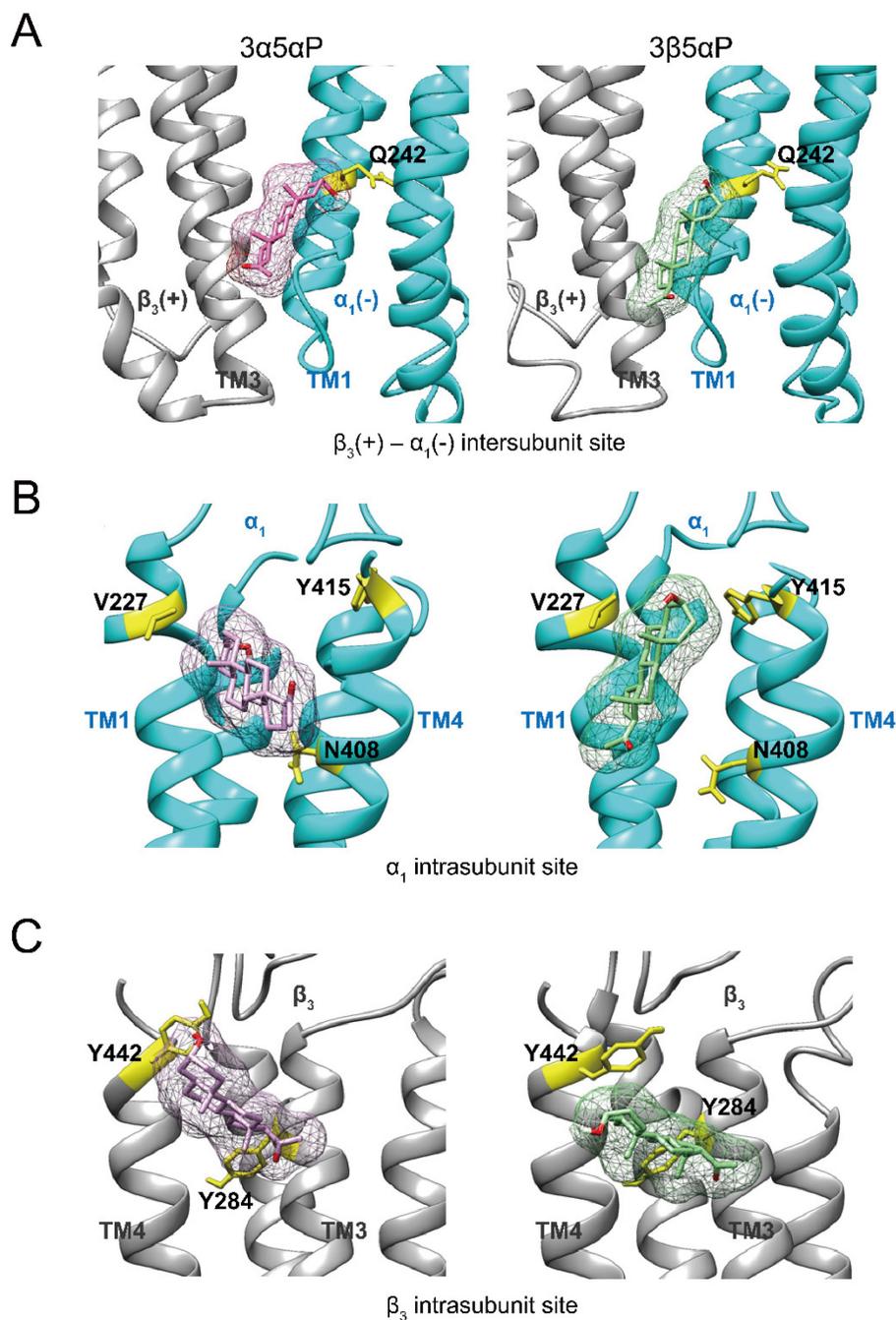
SUPPLEMENTARY FILE 2: **Allopregnanolone and epi-allopregnanolone docking poses within three neurosteroid binding pockets in the $\alpha_1\beta_3$ GABA$_A$R TMD.** (A) Representative poses for allopregnanolone ($3\alpha5\alpha$P) (pink) and epi-allopregnanolone ($3\beta5\alpha$P) (light green) docked within the $\beta_3(+)$–$\alpha_1(-)$ intersubunit site (Vina score: -7.2 for $3\alpha5\alpha$P; -5.9 for $3\beta5\alpha$P). The receptor snapshot is shown along with the α_1Q242 side chain (yellow). (B) Same as (A) for the α_1 intrasubunit site (Vina score: -5.6 for $3\alpha5\alpha$P; -5.8 for $3\beta5\alpha$P). The receptor snapshot is shown along with the α_1V227, α_1Y415 and α_1N408 side chains. (C) Same as (A) for the β_3 intrasubunit site (Vina score: -4.0 for $3\alpha5\alpha$P; -3.6 for $3\beta5\alpha$P). The receptor snapshot is shown along with the β_3Y284 and β_3Y442 side chains.

	Potentiation response ratio		Reduction of potentiation in the presence of competitor (%)	# Cells
	0.1 μM 3α5αP alone	+ 1 μM competitor		
3α5αP vs. KK148	5.1 ± 2.0	4.0 ± 1.2	24 ± 16	6
3α5αP vs. KK150	6.4 ± 2.1	5.8 ± 1.9	12 ± 3	5

SUPPLEMENTARY FILE 3: **KK148 and KK150 decrease allopregnanolone-induced potentiation.** Neurosteroid potentiation of $\alpha_1\beta_3$ GABA$_A$Rs in *Xenopus laevis* oocytes is expressed as potentiation response ratio, calculated as the ratio of the peak responses in the presence of GABA and 0.1 μM allopregnanolone (3α5αP) to the peak response in the presence of GABA alone. The GABA concentrations were selected to generate a response of 3–9% of the response to saturating GABA (30 μM). Co-application of KK148 or KK150 reduces the potentiating effect of 3α5αP on GABA-elicited currents. Data are shown as mean ± SD.